A PRACTICAL FINITE ELEMENT MODEL OF TSADWA TYPE SEMI-RIGID CONNECTIONS FOR PUSH-OVER ANALYSIS OF STEEL FRAMES IN SAP2000

A Thesis Submitted to
the Graduate School of Engineering and Sciences of
İzmir Institute of Technology
in Partial Fulfillment of the Requirements for the Degree of

MASTER OF SCIENCE

in Civil Engineering

by
Öncel ŞEKER

December 2021

İZMİR

ACKNOWLEDGEMENTS

I would like to express my deep and sincere gratitude to my research supervisor, Assoc. Prof. Dr. Engin Aktaş, for giving me the opportunity to do research and providing invaluable guidance throughout this research. His dynamism, vision, sincerity, and motivation have deeply inspired me. He has taught me the methodology to carry out the study and present the research works as clearly as possible. It was a great privilege and honor to work and study under his guidance. I am incredibly grateful for what he has offered me. I would also like to thank him for his friendship, empathy, and great sense of humor.

To my graduate thesis advisory committee, Assoc. Prof. Dr. Emre Ercan and Asst. Prof. Dr. Korhan Deniz Dalgıç. Collectively, I would like to thank them for challenging my knowledge and guiding the research as my thesis developed. Individually, I would like to thank, with his 3-D based finite element analysis expertise, Assoc. Prof. Dr. Emre Ercan for consistently encouraging me to think of how the study should be expanded to be more inclusive and how this work helps me as an engineer for the rest of my life. And I would like to thank Asst. Prof. Dr. Korhan Deniz Dalgıç, for his interest in my thesis, helps me keep perspective on my research fits into the bigger picture. I would also like to thank my external committee: Assoc. Prof. Dr. Sadık Can Girgin and Asst. Prof. Dr. Mehmet Alper Çankaya. Thank you for participating in my defense, and thank you in advance for helping me strengthen my thesis.

I am incredibly grateful to my parents for their love, caring, and sacrifices to educate and prepare me for my future. I am very much thankful to my wife for her love, understanding, continuing support to complete this research work.

Finally, my thanks go to all the people who have supported me to complete the research work directly or indirectly.

ABSTRACT

A PRACTICAL FINITE ELEMENT MODEL OF TSADWA TYPE SEMI-RIGID CONNECTIONS FOR PUSH-OVER ANALYSIS OF STEEL FRAMES IN SAP2000

In steel structural analyses, beam to column connections is traditionally fully pinned or fully rigid. In the analysis assumption, moment (rigid) connections are assumed not to undergo rotation, and shear (pinned) connections can't transfer moment. These classifications do not represent actual connection behavior. Moment (rigid) connections have some relative flexibilities to rotate, and shear (pinned) connections have some capacity to transfer moment. In the light of these actual connection capabilities, another type of connection called partially restrained (PR) or semi-rigid connection is introduced. This study focuses on the behavior of bolted top, and seat angle with double web angle (TSADWA) connection using finite element method (FEM) software (ANSYS) to obtain moment-rotation curves, including geometrical and mechanical properties of the connection and adaptation of the PR connection behavior into the planar frame is performed for performance analysis through SAP2000 software by considering current codes and literature. Azizinamini's (Azizinamini, 1985) experimental and Frye and Morris's (Frye & Morris, 1975) mathematical moment-rotation curves are used to compare with the curves produced in the ANSYS to validate the feasibility of the finite element based PR connection models. A portal frame model with an 8S10 PR connection in the SAP2000 for performance analysis is also compared with the ANSYS portal frame model to demonstrate the correlation between the push-over analyses to reduce the margin of error. Although there is a lack of experimental information on the TSADWA connected frame models, results show that semi-rigid connection models and their usage on the steel frames can propose a reliable and practical methodology for the analysis process.

ÖZET

ÇELİK ÇERÇEVELERİN SAP2000'DE İTME ANALİZİ İÇİN ÜAKGÇK TİPİ YARI RİJİT BAĞLANTILARIN PRATİK BİR SONLU ELEMAN MODELİ

Çelik yapı analizlerinde, kiriş-kolon bağlantıları geleneksel olarak tamamen pimli veya tamamen rijit olarak kabul edilir. Analiz varsayımında, dönmeye izin vermeyen moment (rijit) bağlantıları ve moment aktarmayan kesme (pimli) bağlantıları kullanılır. Bu sınıflandırmalar gerçek bağlantı davranışını temsil etmez. Aslında, moment (rijit) bağlantıların göreli dönme esneklikleri varken, kesme (pimli) bağlantıların moment aktarma kapasiteleri vardır. Bu gerçek bağlantı davranışı ışığında, kısmen kısıtlı veya yarı rijit bağlantı olarak adlandırılan başka bir bağlantı türü tanıtılmıştır. Bu çalışma; cıvatalı üst, alt ve gövdede çift korniyerli (ÜAKGÇK) yarı-rijit bağlantının geometrik ve mekanik özelliklerini içeren moment-dönme eğrilerini sonlu eleman yazılımı (ANSYS) ile oluşturmaya, bu eğrileri düzlemsel çerçeveler üzerinde kullanarak çelik çerçevelerin performans kapasitelerini elde etmeye dayanmaktadır. Gerçekleştirilen çerçeve analizleri, güncel yönetmelikler ve literatür bilgisi dikkate alınarak statik itme analiz yöntemi ile SAP2000 yazılımı aracılığıyla yapılmıştır. Bu süreç içerisinde, Azizinamini'nin (Azizinamini, 1985) deneysel, Frye ve Morris'in (Frye & Morris, 1975) matematiksel moment-dönme eğrileri sonlu eleman yazılımı (ANSYS) kullanılarak oluşturulan bağlantı modellerinin uygulanabilirliğini teyit etmek için kullanılmıştır. Performans analizi için 8S10 bağlantılı yarı-rijit bir portal çerçeve SAP2000 yazılımında modellenerek ANSYS yazılımında oluşturulan çerçeve modeli ile karşılaştırılmış, bu modeller arasındaki bağlılaşım irdelenerek hata payını azaltmak amaçlanmıştır. Çerçeve analizleri ile ilgili deneysel verilerin yokluğuna rağmen elde edilen sonuçlar yarı-rijit bağlantıların sonlu elemanlar aracılığıyla modellenebileceğini ve bu modellerin çerçeve analizleri içerisinde kullanılabileceğini göstermekte, analiz süreci için pratik ve güvenilir bir metodoloji önermektedir.

TABLE OF CONTENTS

LIST OF FIGURES

Figure **Page**

Figure **Page**

Figure **Page**

LIST OF TABLES

LIST OF SYMBOLS AND ABBREVIATIONS

2-D	Two Dimensional
3-D	Three Dimensional
AISC	American Institute of Steel Construction
ASTM	American Society for Testing and Materials
ATC	Seismic Evaluation and Retrofit of Concrete Buildings
ASD	Allowable Stress Design
α	Stiffness Ratio of Connection to Beam
b	flange width of the beam
β	Plastic Moment Capacity Ratio of Connection to Beam
BCs	Boundary Conditions
CP	Collapse Prevention
C1, C2, C3	The Constants for the Polynomial Model
d_b	The diameter of the Bolts
d, h_d	The Beam Depth
E	Modulus of Elasticity
E_c	Modulus of Elasticity of the Column
Et	Tangent Modulus
ε_1, ε_2	The top and bottom flange horizontal displacements, relatively
F_y	Yield Stress
F_u	Ultimate Stress
FR	Fully Restraint
FS	Fully Strength
FEM	Finite Element Model
$F_{pretension}$	Applied Pretension Force
g	The Bolt Gage on the Column Leg of the Connection Angles
h_i	Story Height of j th Floor from Ground
I	Moment of Inertia of the Beam in Major Axis
I_c	Moment of Inertia of the Column in Major Axis
IO	Immediate Occupancy
IMF	Intermediate Moment Frame
K_i	Inıtial Stiffness of the Connection

K_s	Secant Stiffness, Ms/θs
K_t	Tangent Stiffness
K	Standardization Constant for Polynomial Model
K_{beam}	Stiffness of the Beam, (EI/L)
L	The Length of the Beam
L_{angle}, L_c	The Angle Lengths
L_{bay}	Bay Length of Frame
LS	Life Safety
M	The Bending Moment
M_s	Moment of the Connection at Service Loads
M_n	The Connection Ultimate Moment Strength
M_p	The Plastic Moment Capacity of the Beam
M_{yc}	The Yield Moment Capacity of the Connection
M_{pc}	Plastic Moment Capacity of the Connection
M_{uc}	The Ultimate Moment Capacity of the Connection
M_{pb}	Plastic Moment Capacity of the Beam
MDOF	Multi Degree of Freedom
PZ	Panel Zone
PR	Partially Restraint
PS	Partially Strength
p	The Bolt Spacing in the Leg on Column Flange
P_d	The Summation of the Reactions of Applied Displacement on the Beam End Nodes
R_{ki}	Inıtial Stiffness of the Connection
R_{ks}	Secant Stiffness, Ms/θs
R_{kb}	The Connection Stiffness from Origin to Intersection Point of the Beam-Line and Non-Linear Moment-Rotation Curve
R_{kl}	The Leeward Side of the Connection Stiffness
R	The Relative Rotation of the Connection
SMF	Special Moment Frame
SDOF	Single Degree of Freedom
TSADWA	Top and Seat Angles with Double Web Angles
t_c	Flange Thickness of the Column
$V_{pz,h}$	Horizontal Shear Force in Panel Zone Region

$V_{pz,v}$	Vertical Shear Force in Panel Zone Region
θ	The Rotation
θ_s	Rotation of the Connection at Service Loads
θ_u	Ultimate Rotation Capacity of the Connection
θ_{yc}	The Yield Rotation Capacity of the Connection
θ_{pc}	The Plastic Rotation Capacity of the Connection
θ_{uc}	the Ultimate Rotation Capacity of the Connection
δ	Deformations Along with the Members, Measured Relative to the Member Chord
Δ	Measured Story Drifts between Member Ends in Buildings

CHAPTER 1

INTRODUCTION

1.1. General

Each earthquake brings different lessons to the profession of earthquake engineering. One of the main lessons of the Northridge (1994) earthquake was the extensive and unanticipated damage to welded steel moment-resistant frame structures. Although no casualties were reported related to that problem, countless welded steel beams to column connections were observed with the brittle nature of the fractures.

Before the earthquake in Northridge (1994), engineers and codes intended to make the connections had excellent moment capacity under the forces coming from earthquake movements (Mahin, 1998). However, after achieving their capacities, these kinds of connections failed in a brittle way, causing severe damage to these structures. One of the lessons learned from the post-earthquake reconnaissance reports is that moment capacity is not the only criterion for structural connections in earthquake-resistant steel structures. The connections should have energy dissipation capabilities and adequate moment capacity to effectively resist the forces of the earthquake with sufficient ductility form (Nguyen & Kim, 2014; Elnashai & Elghazouli, 1994).

For the sake of simplicity, most design engineers accept connections with the assumption of a perfectly rigid or ideally pinned connection behavior. The perfectly rigid connection assumption prohibits rotation between the connected parts and transfers the end moment to the other. On the other hand, an ideally pinned connection permits the connected components to rotate relative to one another, and moment transfer is negligible. Although the popularity of these simplified models comes from their convenience of design and analysis of steel framing systems, this simplification may result in erroneous frame behavior assessment. In reality, each connection's actual behavior falls somewhere between two idealized extremes. These actual connections, called semi-rigid connections, have moment capacity and some rotational capability, which might provide sufficient energy dissipation to resist earthquake demands.

Moment-rotation diagrams illustrate the behavior of structural connection elements and their interaction with each other in the best way since the moment-rotation curves contain relatively movement of connection region with the column, beam, and connection capacities. Because the rotation of the beam members in a physical test is often measured across a length that includes the contributions of the connecting components and the ends of the connected members and the column panel zone, the connection response is described in this way. The moment-rotation curves of these combinations show a nonlinear behavior (AISC 360-16, 2016).

Today, in terms of sustainability concerns, the economic solution of construction systems is gaining significance. In the research of rigid and semi-rigid joints, optimum designs of semi-rigid steel frames are compared with optimum designs of rigid steel frames; semi-rigid steel frames have been shown to offer more cost-effective outcomes (Weynand, Jaspart, & Steenhuis, 1998).

The fact that these connections are cost-effective in steel frame construction and efficient at energy dissipation for earthquake response does not automatically make them popular since the nonlinear behavior of semi-rigid connections in practical design applications is a complex operation. However, with the help of computer technology, thorough modeling and analysis of structures using advanced finite element software are very widespread. Especially, reasonably accurate behavior estimation of that structure is a matter of interest for the designer or researcher.

1.2. Types of Semi-Rigid Connections

In modern and industrial practice, steel frame systems are extensively preferred. However, there is still some room for improvement in designing those structures. For example, relaxing the idealizations such as fully rigid or ideally pinned connections, which limit taking full advantage of using steel framing, may allow reaching more economical designs. An over simplified approach would be preferable purposes when you don’t have the appropriate tools to handle it properly. But it would be missing opportunities not to utilize them once you have. Therefore, effective analysis and design of connections become important points. Capabilities of its actual behavior can provide more reliable and economical designs (Haapio & Heinisuo, 2010; Weynand, Jaspart, & Steenhuis, 1998). In the literature, lots of studies were published on semi-rigid

connections. According to experimental data collected so far are mostly classified into seven types of semi-rigid connection as seen in Figure 1.1 (Chen, Kishi, & Komuro, Semi-Rigid Connections Handbook, 2011).

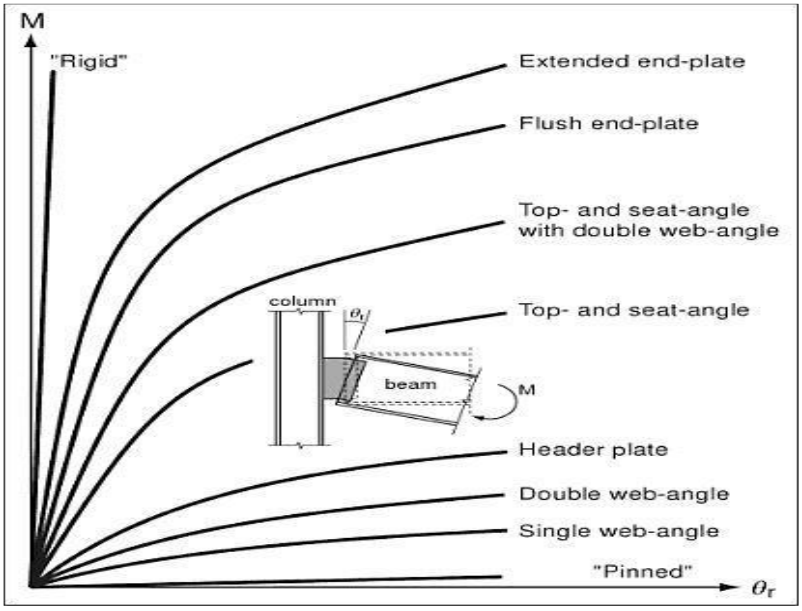

Figure 1. 1 Typical Moment-Rotation (M–θ) Curves of the Beam-to-Column Connections

(Source: (Chen, Kishi, & Komuro, 2011))

This thesis will focus on top and seat with double web angles (TSADWA) connection due to its increasing use in practice and also increasing interest in the research community because of its semi-rigid features in terms of stiffness, strength, and ductility.

1.2.1. Single Web–Angle / Plate Connections

As appeared in Figure 1.2, single web-angle connections include an angle either bolted or welded to the column flange and the beam web. Contrarily, single plate connections use the plate instead of the angle, as shown in Figure 1.3. The single web-angle connections have a moment rigidity equal to approximately one-half of the double web-angle connections, and the single plate connections have moment rigidity equal to or greater than the single web-angle connections since one side of the plate is completely welded to the column flange (Chen, Kishi, & Komuro, 2011).

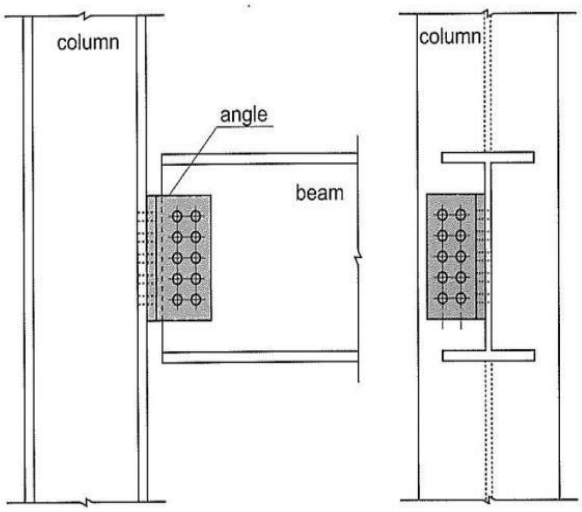

Figure 1. 2 Single Web-Angle Connection

(Source: (Chen, Kishi, & Komuro, 2011))

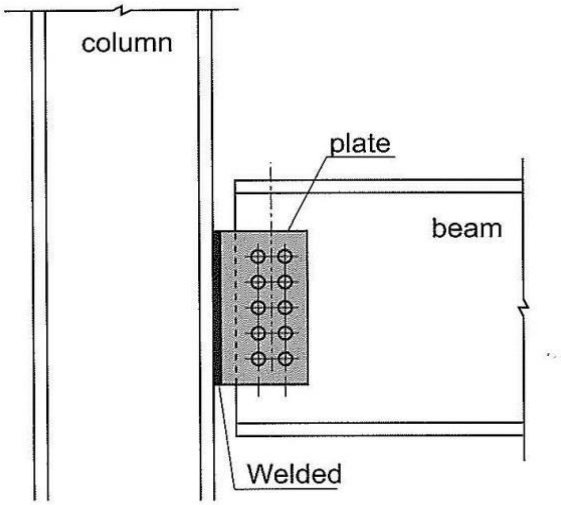

Figure 1. 3 Single Plate Connection

(Source: (Chen, Kishi, & Komuro, 2011))

1.2.2. Double Web-Angle Connections

Double web-angle connections consist of two angles, either bolted or riveted to both the column and the beam web, as illustrated in Figure 1.4. Nowadays, high-strength

bolts are utilized popularly as fasteners for this type of connection. The connection is stiffer than those of single web-angle and single plate connections (Chen, Kishi, & Komuro, 2011).

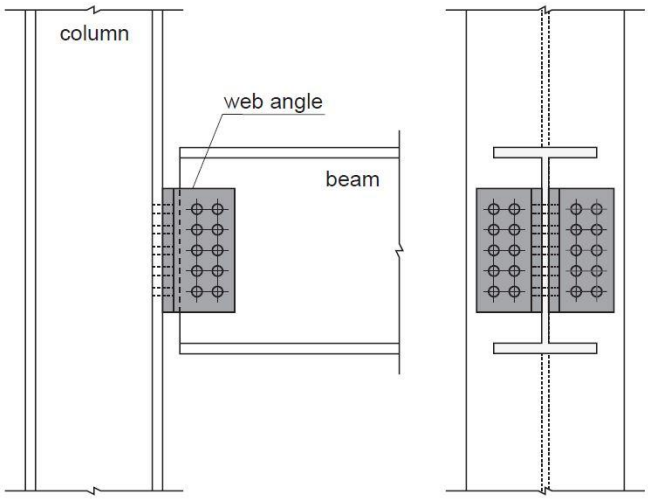

Figure 1. 4 Double Web-Angle Connection

(Source: (Chen, Kishi, & Komuro, 2011))

1.2.3. Top- and Seat-Angle Connection

The type of top and seat angle connection, as displayed in Figure 1.5, has two angles that fasten beam flanges to column flanges with bolts. The aim of these angles was represented in two major points as follows that the top angle is used to supply horizontal support of the compression flange of a beam, and the seat angle is used to transfer the vertical shear response of the beam. The column should not present a substantial restraining moment to the end of the beam. These connections can transfer not only the vertical shear reactions but also some end moment of the beam to the column according to the experimental results (Chen, Kishi, & Komuro, 2011).

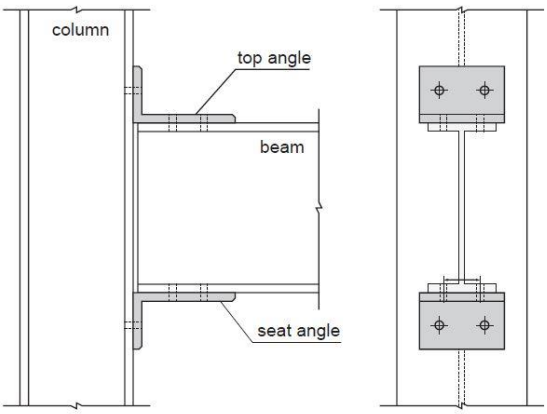

Figure 1. 5 Top and Seat Angle Connection

(Source: (Chen, Kishi, & Komuro, 2011))

1.2.4. Top and Seat Angle with Double Web-Angle Connections

This type of connection is a combination of four angles that assemble the beam to the column through the bolts in top- and seat-angles with web angles, as shown in Figure 1.6. Double web angles increase shear transfer capacity and restraint characteristics of connection compared to the top and seat angle connections. According to AISC-ASD specifications, which were published in 1989, this type of connection is considered "semi-rigid."

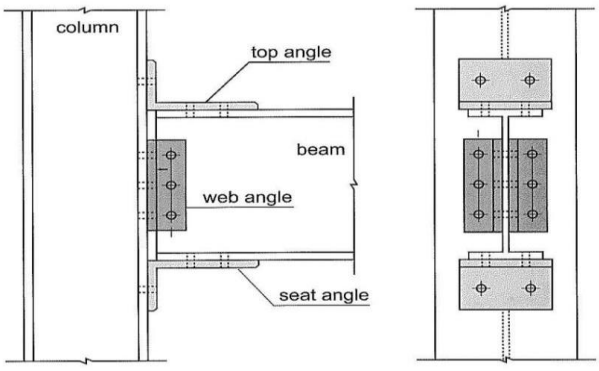

Figure 1. 6 Top and Seat Angles with Double Web Angles Connection Type (TSADWA)
(Source: (Chen, Kishi, & Komuro, 2011))

1.2.5. Extended End-plate Connections/Flush End-plate Connections

An ordinary end plate connection was welded to beam web and flanges in the fabrication phase and bolted the column in the field. As shown in Figures 1.7 and 1.8, the extended end-plate connections are categorized into two end-plate types, either extended on the tension side or both on the tension and compression sides. Some end plate connections can be categorized in FR connection concerning specifications due to their end moment transfer capacity from the beam to the column. A typical flush end-plate connection can be seen in Figure 1.9. The end-plate connection that is flush is weaker than the end-plate connection that is extended. (Chen, Kishi, & Komuro, 2011).

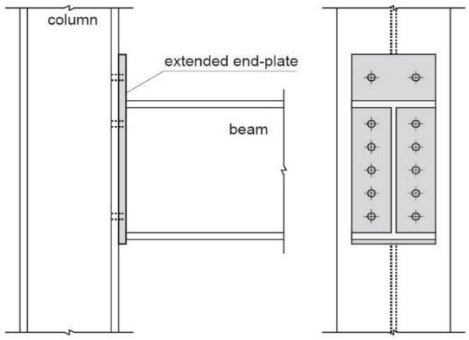

Figure 1. 7 Extended End-Plate Connection Only on the Tension Side

(Source: (Chen, Kishi, & Komuro, 2011))

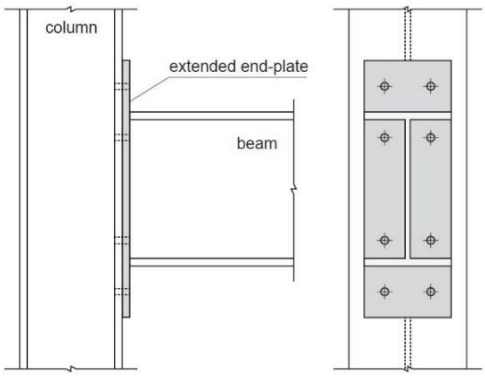

Figure 1. 8 Extended End-Plate Connection on Both Tension and Compression Sides

(Source: (Chen, Kishi, & Komuro, 2011))

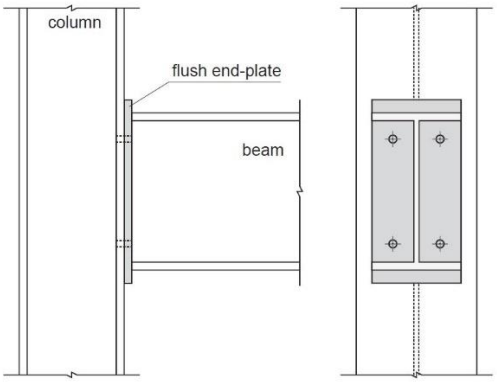

Figure 1. 9 Flush End Plate Connection

(Source: (Chen, Kishi, & Komuro, 2011))

1.2.6. Header Plate Connections

A header plate is considered an endplate connection that does not cover the whole beam depth, as shown in Figure 1.10. This type of connection consists of an endplate with fillet welds to beam web on each side in the fabrication stage and with bolts on the field to column flange. The moment-rotation characteristics of header plate connection are similar to double web-angle connection. On the other hand, this connection has shear transfer capacity from beam end to column instead of moment resistance capacity. Therefore, it is generally considered a pinned connection according to specifications.

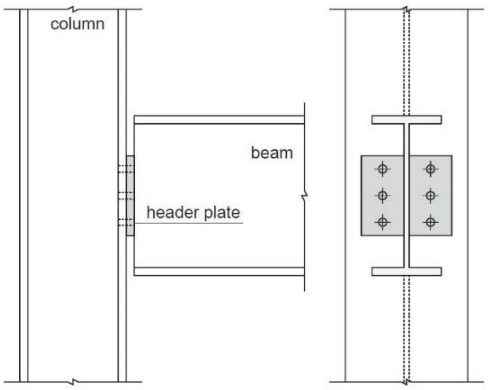

Figure 1. 10 Header Plate Connection

(Source: (Chen, Kishi, & Komuro, 2011))

1.2.7. Literature Review of TSADWA Semi-Rigid Connection

TSADWA connection type was first mentioned in 1936 by Rathbun (Chen, Kishi, & Komuro, 2011) with experimental research, which presents itself as a more ideal partially restrained connection among the others as seen in Figure 1.1. Therefore, many researchers, in time, adopted this connection type to examine the behavior of the semi-rigid connection. In 1985 at the University of South Caroline, Azizinamini's (Azizinamini, 1985) detailed experimental Ph. D. study was reported. In the study, 20 specimens of TSADWA connection were performed based on the variables, mainly section dimensions of the connection elements and bolt properties.

Azizinamini has mostly investigated static loading conditions besides cyclic loading conditions. He converted load-deformation curves, which are obtained from test equipment, into moment-rotation curves. The curves were compared with analytical and empirical mathematical models to show their relation to each other. In past decades many researchers used these test data to comprehend the nature of PR connection and to explain uncertainties of test conditions that are not explicitly stated in the study. The practical calculation and modeling process of the connection was developed by using FEM analysis with a comparison of mathematical models (Citipitioglu, Haj-Ali, & White, 2002; Pirmoz & Gholizadeh, 2007; Pirmoz & Danesh, 2009; Danesh, Pirmoz, & Daryan, 2006).

In the light of experimental data and computer-based analysis with mathematical approaches, understanding of connection behavior make researchers enthusiastic to carry out semi-rigid connection into the frame design. Although earlier AISC editions and studies are performed with the initial slope of connection stiffness value, Ki, only a small part of the curve is represented with that linear range. The great part of the semi-rigid connection behavior is non-linear (Leon, 2017). Today, secant and tangent stiffness are more commonly used in advanced analysis programs that can handle non-linear or multi-linear rotational spring definitions. In several studies, linearized stiffness, Ks, that is obtained from moment-rotation curve according to AISC specifications analyzed on the frame to change ordinary steel design approach by taking semi-rigid connection effects into account (Surovek, White, & Leon, 2005; Singh & Lui, 2014; Chen & Lui, 1991). The research process that progresses over time revealed detailed frame analysis starting from linear first or second-order analysis to performance-based earthquake analysis. In other words, from force-based analysis to displacement-based analysis under dynamic

forces. However, seismic design is still a complex topic due to the lack of getting detailed experimental data for the semi-rigidly connected frame cases, although advanced analysis methods have been provided. Even if publications present a robust starting point to model PR connection and AISC specifications or FEMA-356 specifies boundaries, both ductility and energy dissipation capacity have to be understood clearly for a proper and efficient design due to the unfamiliar case of PR connection model to designer.

The general scope of semi-rigid or PR connection types has been an area of interest since the 1940s in the AISC specifications (Leon, 2017). Therefore, a huge number of researches have been published that have addressed different parts of the connection property, which is not possible and meaningful to mention as a whole. For this reason, this section presents the studies from researchers who are commonly focused on the finite element-based semi-rigid connection models and their usage in the steel frame analyses.

Citipitioglu et al. (2002) conducted a detailed finite element analysis on TSADWA connections with the ABAQUS software program by using Azizinamini's experimental research. The study enlightened some missing information that was not mentioned in the experimental study, such as bolt material properties and pretension values. Fixed pretension loads, contact surfaces, and friction coefficients were determined to match the numerical study closely experimental one. This thesis introduced pretension and friction values within the operation range, and some modeling assumptions were adopted to reduce analysis time.

In A. Pirmoz's (2006) paper, the moment-rotation behavior of top and seat bolted angle connections with double web angles is studied using finite element modeling and neural networks. Azizinamini's tests were chosen to examine the effects of different geometric properties of connection such as top and web angle dimensions and bolt spacing on connection behavior. Firstly, test results were used to train a neural network for prediction moment-rotation curves. Then, predicted curve and parametric finite element analysis were performed, and results were plotted. The study presents a good agreement of models. Therefore, the research provides reduced computational time of finite element analysis by giving parametric analysis opportunities on geometrical and mechanical connection properties.

Abdalla (2015) studied the failure behavior of a top and seat angle connection with double web angles that had been related to static loading. A three-dimensional nonlinear finite-element model was developed to demonstrate the real rotational behavior

of the structure, including opening and/or sliding among connected parts. Experimental test results were conducted on the connection for validation of finite element models, and then validated computational models were used to investigate critical components of the connection, such as the top angle, and those failure modes were presented based on parametric analysis.

Lui and Chen (1986) published an analysis of the earliest research on flexible joint frames. A method for analyzing the behavior of plane steel frames was presented. The analysis was based primarily on the formulation of beam-column and connection elements. For the modeling of geometric non-linear elastic beam-column element updated Lagrangian approach has been adopted. For the modeling of other elements, the exponential function was used to represent the non-linear behavior of connection in terms of moment and rotation. The study concludes that the connection has a significant effect on the overall stability and ultimate resistance capacity of steel frames. Assumptions of fully rigid and ideally pinned connections are just design simplifications. Most connections illustrate between these two extreme cases.

Elnashai and Elghazouli (1994) performed elaborated research on the seismic behavior of semi-rigid steel frames in comparison with the rigid alternatives. Half of the two-story single-bay TSADWA semi-rigid and fully welded rigid connection of frame test set-up used to provide detailed information under monotonic, cyclic, and pseudo-dynamic earthquake loading conditions. Advanced non-linear analysis program used for modeling to analytical studies. The analytical model was utilized to examine the influence of connection type on the seismic response capacity of members and frames. The study showed both experimental and analytical models of PR connection frame had enough earthquake resistance capacity with its ductile and stable hysteretic behavior.

Lei Xu (2001) presented an analysis method that specifically considered both the nonlinear rotational behavior of beam-to-column connections and the second-order effects of the beam-column members. In research, the concept of an end-fixity factor, r, was elaborately introduced to assign connection rigidity that is related to the connection stiffness ratio. The end-fixity factor, r, covers the nonlinear nature of connection in approximately linear range and gives physical interpretation to the researcher. With this concept, the end rotational condition was simplified in definition range that has a value from zero to one without considering the direct classification of rigid, pinned, or semi-rigid connections. In addition, the end fixity factor simplifies the analysis procedure for semi-rigid frames. Thus, the proposed analysis method, including the end fixity factor,

was performed for first and second-order elastic analysis, and an iterative procedure was used to count the nonlinear behavior of the connection in the member stiffness matrix. The researcher aimed to illustrate the validity and efficiency of the proposed approach with examples.

Singh and Lui (2013) proposed a design technique for PR frames that consider the semi-rigid nature of connections, counting their loading/unloading behavior under combined gravity and wind loads. TASDWA connections were displayed utilizing the three-parameter analytical model to provide the proposed design method. For simplification of the design, two linearized connection stiffness values were calculated based on anticipated connection loads. The analysis is conducted utilizing the AISC direct analysis method.

In the proposed design procedure, according to AISC, a TSADWA connection was classified in a semi-rigid range with its secant stiffness ratio that falls between $2<R_{ks}(L/EI)<20$ under service loads. Then intersection point of the beamline and non-linear moment-rotation curve was constructed, and a line was drawn from origin to this point that was defined as connection stiffness, R_{kb}, under factored gravity loads. Lateral wind load on the PR connection was conducted as the windward side of the frame consisted of unloading connection, R_{ki}, and leeward side consisted of loading connection, R_{kl}. The proposed method is validated by using the direct analysis method on examples of these connection approaches.

1.3. Connection Classification

Moment-rotation (M-θ) curves are usually considered the best representation of the connection behavior for design purposes. These curves of M-θ are typically derived from experimental specimens. The moments (M) are determined directly from the specimen statics, and the rotations (θ) are calculated over a distance usually equal to the beam depth, as shown in Figure 1.11a. The observed rotation thus covers both elastic and inelastic components of deformation that exist in the joint area also provide the portion of beam and the column panel zone.

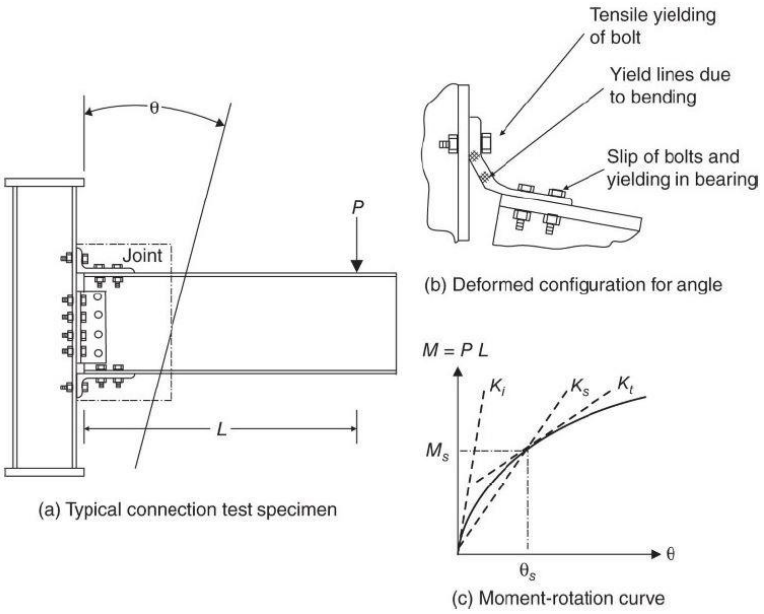

Figure 1. 11 Derivation of the Moment-Rotation Curve from Experiments

(Source: (Leon, 2017))

A typical example of the deformed shape of these components that are incorporated in the moment-rotation curve by considering its whole behavior is demonstrated in Figure 1.11b. Several stiffness parameters were adopted to classify connections from past years to the present in design codes. Figure 1.11c illustrates these slopes of the lines as initial, K_i, secant, K_s, and tangent, K_t, stiffness on the moment rotation curve.

The classification of connections is handled with three stages in design codes (AISC 360-16, 2016; FEMA-356, 2000; AISC 341-16, 2016). These specification parameters are as follows:

- Strength
- Ductility
- Stiffness

The contribution of these parameters can be explained by the help of AISC Specification to classify connections for Structural Steel Buildings.

1.3.1. Strength

The ultimate strength of connection, M_n, which is demonstrated in Figure 1.12, can be specified on the basis of the ultimate limit state model of connection or from physical tests. If the moment-rotation response does not provide a peak load, then the strength can be taken as the moment at a rotation of 0.02 rad (AISC 360-16, 2016). The connection strength parameter for classification is defined as either full strength or partial strength connection depending on the comparison of the beam full plastic strength, $M_{p,\ beam}$. If the beam full plastic strength, M_p, exceeds the ultimate connection strength, M_n, the connection is partial strength (PS), otherwise full strength (FS). Also, connections that are not able to carry at least %20 of $M_{p,\ beam}$ at rotation 0,02 rad is considered to have no flexural strength (AISC 360-16, 2016) (Leon, 2017). These classifications of definitions are summarized below

Table 1.1 Strength-Based Connection Classification

A connection is a full-strength (FS) if $M_n \geq M_{p,\ beam}$
A connection is a partial strength (PS) if $M_n \leq M_{p,\ beam}$
A connection has no flexural strength if it has a capacity less than $0.2\ M_{p,\ beam}$

1.3.2. Ductility

When the connection strength greatly overtakes the fully plastic moment strength of the beam, the ductility of the structural system is managed by the beam, and the connection is considered elastic. If the connection strength exceeds the maximum plastic moment strength of the beam just slightly, the connection can undergo significant inelastic deformation before the beam reaches its limit strength. If the beam strength is higher than the connection strength, then deformations can intensify in the connection (AISC 360-16, 2016). Therefore, the ductility of the connection in the case of partial strength (PS) connection is a significantly important parameter, as appeared in Figure 1.13. The rotation capacity, θ_u, can be determined as the value of the connection rotation at the point where either the resisting strength of the connection has dropped to $0{,}8M_n$ (Figure 1.12) or the connection has deformed beyond 0,03 rad (Figure 1.13) (AISC 360-

16, 2016). Consideration of ductility for the seismic design according to AISC 341-16, the rotation, θ_u, is equal or greater than 0,02 rad in intermediate moment frame (IMF), and the rotation, θ_u, is equal or greater than 0,04 rad in special moment frame (SMF).

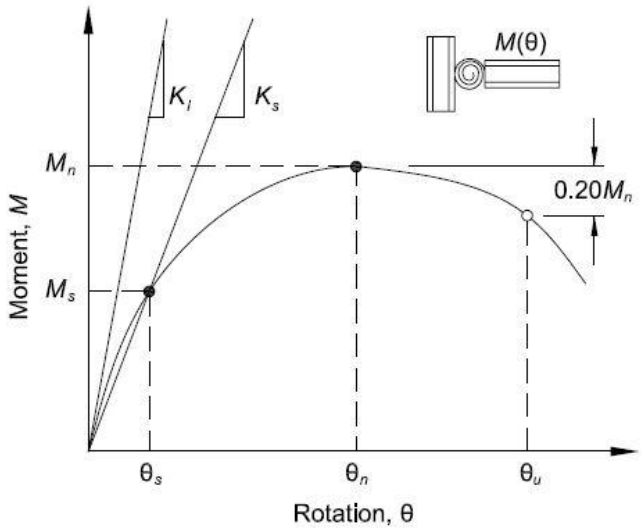

Figure 1.12 Definition of Stiffness, Strength, and Ductility Characteristics of the Moment-Rotation Response of a Partially Restrained Connection.

(Source: (AISC 360-16, 2016))

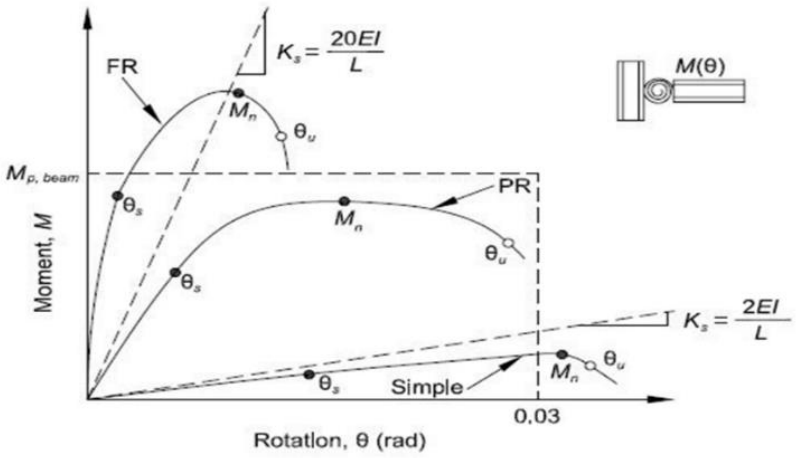

Figure 1. 13 Classification of the Moment-Rotation Response of Fully Restrained (FR), Partially Restrained (PR), and Simple Connections.

(Source: (AISC 360-16, 2016))

1.3.3. Stiffness

As mentioned earlier, the connection stiffness is usually taken as the slope, R_{ks}, of the moment-rotation curve. Most of the connections illustrate nonlinear behavior even at low moment rotation values. Therefore, it is an easy way to define stiffness value with the tangent approach, as shown in Figure 1.11c. Initial connection stiffness, K_i, doesn't represent the connection response properly at the service load level. In addition, several types of connections do not display a consistent initial stiffness and occur only for a very limited moment range. Hence, the secant stiffness, K_s, at service loads is taken as a reasonable connection stiffness value for a regular frame design (AISC 360-16, 2016; Leon, 2017). Secant stiffness, K_s, is defined as R_{ks} that M_s is divided by θ_s as shown in Figure 1.12, where M_s moment at service load level and θ_s rotation at service load level. The stiffness of the connection is purposeful when compared to the stiffness of the connected members. Therefore, connection classification with stiffness values is related to beam rigidity, as summarized in Table 1.2 and appeared in Figure 1.13.

Table 1.2 Stiffness-Based Connection Classification

$R_{ks}.(L/EI)_{beam} > 20$, A connection is fully restrained (FR),
$2 \leq R_{ks}.(L/EI)_{beam} \leq 20$, A connection is partially restrained (PR),
$R_{ks}. (L/EI)_{beam} < 2$. A connection is simple.

1.4. Objective and Organization of Thesis

In this thesis, finite element analysis of semi-rigid connection through 3-D solid finite element model and its efficiency on a structural steel frame is studied. Azizinamini's experimental research for semi-rigid connection, namely the top-seat angles with double web angles, was chosen during the thesis process. Analysis results for the FE models with the test results of their related specimens are compared. Then, a simplified mathematical model to represent the actual behavior of the TSADWA semi-rigid connection is investigated for practical usage on steel frame design. For the selected

mathematical approach, literature is extensively researched to specify the type of connection subject to the thesis successfully. The purpose of the overall process is to propose practical methodology with reliable results by using finite element-based software effectively for modeling and analysis procedures without needed experimental studies.

There are five chapters in this thesis. The first chapter begins with a general introduction and moves on to information on the steel connection types and a review of experimental and numerical research on top and seat angles with double web angle (TSADWA) connection and ends with connection classification knowledge based on AISC360-16.

The second chapter explains how to simulate the beam-to-column connection region with bolts, pretension, contacts, friction, and material and geometric nonlinearities using ANSYS finite element software. The types of material models used in ANSYS are described, followed by detailed instructions on meshing and modeling of bodies and bolts. Illustrations clarify the contact properties and bolt pretension parameters that must be used in the analysis.

The third chapter works with standardized non-dimensional mathematical models created for semi-rigid connections, and their comparison with the current FE study will be discussed, including the experimental results of the connections.

The fourth chapter shows the distinctive steel planar frames that are selected to conduct static push-over analysis with the nonlinear TSADWA connection. In order to demonstrate the efficiency of partially restraint connection on the frame performance, the chosen frame models are compared with its rigidly connected ones.

The last chapter provides a clear description and conclusion of the thesis and a short discussion of potential future research directions on semi-rigid connections.

CHAPTER 2

MODELING AND ANALYSIS OF THE SEMI-RIGID CONNECTION WITH FINITE ELEMENT METHOD

This part presents modeling details, experimental parameters, approximations, and assumptions that are taken from the literature for the non-linear finite element modeling of semi-rigid connections. ANSYS FE analysis software is one of the most popular software among commercial software. This provides enough modeling information to the user for solution strategy. Since simulating a thorough reaction of a steel beam to a column connection region in FE software is still a complicated combination of material, geometry, and contact non-linearities. The software does not only supply easy interface usage, but also it has a relation with popular CAD software. Therefore, the PR model is constructed of the SOLIDWORKS program and is transferred to ANSYS Workbench for displacement-based 3D finite element (FE) analysis.

For the finite element model and analysis, Azizinamini's top and seat angle specimens with double web angles are used (Azizinamini, 1985). A pair of beams are joined to the stub column in the middle by the top and seat angles, which are fastened to the beam and column flanges, and the double web angles, which are attached to both the beam web and the column flanges. Figure 2.1 shows how this arrangement works. To develop an effective moment-rotation response of the TSADWA semi-rigid connection, a three-dimensional model that covers all impacts of a complicated process was used.

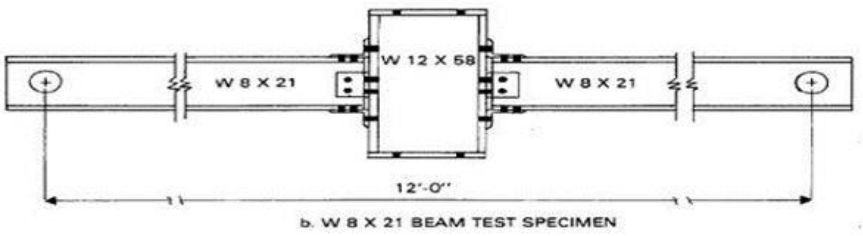

Figure 2. 1 Test Set-up of Azizinamini’s Specimen

(Source: (Azizinamini, 1985))

Even though there are many complexities in the modeling process, such as mechanical and geometrical non-linearities of members, the finite element method still provides a reasonably accurate solution if some approaches are implemented properly in the model. Also, bolt pretension forces and contact surfaces with friction values become an important point to specify the sensitivity of the analysis. However, approximations or assumptions to facilitate analysis must be considered carefully since even if small changes take place, convergence problems or unexpected distinctions can be seen in results. Azizinamini's specimens from 8S1 to 8S10 are performed, and all material and modeling information that is coming from his Ph.D. study or literature is presented below.

2.1. Prior Experimental Research

In Azizinamini's research, two types of semi-rigid connections are taken into consideration. One of them is top and seat with double web angle connection specimens that are used in this thesis, and the other one is top and seat angle without double web angle connection specimens that are not presented with enough tests. Only TSADWA specimens are analyzed with finite element analysis. Herein, Connection parameters are elaborately indicated in Figure 2.2.

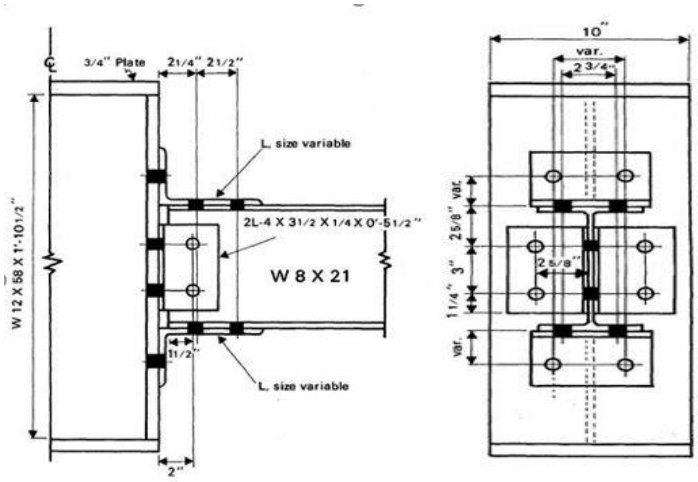

Figure 2. 2 Azizinamini's Test Set-Up Representation with 8S Types Configuration (Source: (Azizinamini, 1985))

The primary connection parts, such as the beam, column flange, and web angles, as well as bolts and nuts, must all be simulated using simple material characteristics and models. The mild carbon steel ASTM A36 used for the main connection elements and ASTM A325 heavy hex high strength bolts and nuts are used with A325 hardened washers in the experimental analysis. 8S type section parameters should be assessed into two categories as constants and variables (as seen in Figure 2.2). Constants are web angle parameters, W8x21 beam, W12x58 column, and those contact places. Variables are angle thicknesses and lengths, bolt diameters and hole places, etc. All section parameters of 8S type test specimens are listed below in Table 2.1.

Table 2. 1 List of Test Specimens (Source: (Azizinamini, 1985))

			Top and Bottom Flange Angles				Web Angles	
Specimen Number	Beam Section	Bolt Diameter	Angle	Length	Gage in the Leg on Column Flange "g"	Bolt Spacing in the Leg on Column Flange "p"	Angle	Length "Lc"
8S1	W8X21	3/4 (19.05)	L 6 X 3 1/2 X 5/16 (152.4 x 88.9 x 7.94)	6 (152.4)	2 (50.8)	3 1/2 (88.9)	2L4 X 3 1/2 X 1/4 2x(101.6 x 88.9 x 6.35)	5 1/2 (139.7)
8S2	W8X21	3/4 (19.05)	L 6 X 3 1/2 X 3/8 (152.4 x 88.9 x 9.53)	6 (152.4)	2 (50.8)	3 1/2 (88.9)	2L4 X 3 1/2 X 1/4 2x(101.6 x 88.9 x 6.35)	5 1/2 (139.7)
8S3	W8X21	3/4 (19.05)	L 6 X 3 1/2 X 5/16 (152.4 x 88.9 x 7.94)	8 (203.2)	2 (50.8)	3 1/2 (88.9)	2L4 X 3 1/2 X 1/4 2x(101.6 x 88.9 x 6.35)	5 1/2 (139.7)
8S4	W8X21	3/4 (19.05)	L 6 X 6 X 3/8 (152.4 x 152.4 x 9.53)	6 (152.4)	4 1/2 (114.3)	3 1/2 (88.9)	2L4 X 3 1/2 X 1/4 2x(101.6 x 88.9 x 6.35)	5 1/2 (139.7)
8S5	W8X21	3/4 (19.05)	L 6 X 4 X 3/8 (152.4 x 101.6 x 9.53)	8 (203.2)	2 1/2 (63.5)	5 1/2 (139.7)	2L4 X 3 1/2 X 1/4 2x(101.6 x 88.9 x 6.35)	5 1/2 (139.7)
8S6	W8X21	3/4 (19.05)	L 6 X 4 X 5/16 (152.4 x 101.6 x 7.94)	6 (152.4)	2 1/2 (63.5)	3 1/2 (88.9)	2L4 X 3 1/2 X 1/4 2x(101.6 x 88.9 x 6.35)	5 1/2 (139.7)
8S7	W8X21	3/4 (19.05)	L 6 X 4 X 3/8 (152.4 x 101.6 x 9.53)	6 (152.4)	2 1/2 (63.5)	3 1/2 (88.9)	2L4 X 3 1/2 X 1/4 2x(101.6 x 88.9 x 6.35)	5 1/2 (139.7)
8S8	W8X21	7/8 (22.225)	L 6 X 3 1/2 X 5/16 (152.4 x 88.9 x 7.94)	6 (152.4)	2 (50.8)	3 1/2 (88.9)	2L4 X 3 1/2 X 1/4 2x(101.6 x 88.9 x 6.35)	5 1/2 (139.7)
8S9	W8X21	7/8 (22.225)	L 6 X 3 1/2 X 3/8 (152.4 x 88.9 x 9.53)	6 (152.4)	2 (50.8)	3 1/2 (88.9)	2L4 X 3 1/2 X 1/4 2x(101.6 x 88.9 x 6.35)	5 1/2 (139.7)
8S10	W8X21	7/8 (22.225)	L 6 X 3 1/2 X 1/2 (152.4 x 88.9 x 12.7)	6 (152.4)	2 (50.8)	3 1/2 (88.9)	2L4 X 3 1/2 X 1/4 2x(101.6 x 88.9 x 6.35)	5 1/2 (139.7)
All parameters in inches (mm).								

These parameters express the angle thickness (t), angle lengths (L_{angle} and L_C), bolt diameters, spacing (p), and the bolt gage on the column leg of the connection angles (g).

The flange and web angles were connected to the beam sections with the same diameter bolts used to connect to the column flange in the all-bolted examples. In Azizinamini's study, heavy column sections were chosen to remove the column panel zone effect as a contributing behavior factor, restricting the moment-rotation interaction to the connecting elements, and his test configuration was composed of the thick flanged column which is resulted from no or little plastic yielding during the testing process (Azizinamini, 1985). Beams were also chosen to ensure that no plastic deformation occurred in the section. By using this method, the connection had failed before the beam element yielded or any plastic deformation occurred. The identical beam and column section was used throughout all tests when no plastic deformation was noticed in the column and beam sections during testing. Thus, the effects of using different top and seat angle sections on connection and moment-rotation curves were examined and submitted in Azizinamini's study (Azizinamini, 1985).

2.2. Finite Element Model

Three-dimensional FE models are aimed to perform the moment–rotation response of the semi-rigid connections. Therefore, Azizinamini's experimental work and test results are modeled to indicate this aim. And also, the main goal of using experimental data here is to model the connection accurately to reveal that a semi-rigid connection can now be used without the need for experimental data. Through the modeling process in ANSYS, some assumptions and missing information that was not provided from the experimental research is completed from literature, as mentioned before. This complementary literature information provides less consuming time to the researcher for the analysis through the efficiency of the commercial software.

Although connections experience axial, shear, and torsion deformations, they are usually small compared to rotational deformation. The researchers often observe only the connection's rotational deformation in assessing frame response. In the FE model, the beam movement was released only in the flexural deformation direction. Also, the column flanges and web region were thought of as stiff enough to neglect the panel zone (PZ)

effect as was demonstrated in the experimental study's results and also in the portal frame example of this study through the ANSYS FEM. Therefore, it can also be considered that when both strength and stiffness criteria are provided, direct modeling of panel zone shall not be required according to FEMA-356 (FEMA-356, 2000; Miri & Naghipour, 2009). Thus, boundary conditions and assumptions that facilitate the modeling process was specified to focus connection part solely as follows: (1) half of the overall test setup is modeled by the help of symmetry about the other half, (2) only the column flange part is modeled in the connection simulation and, (3) the flange part of the column is modeled to fix back of its surface against deformations (Citipitioglu, Haj-Ali, & White, 2002; Pirmoz & Gholizadeh, 2007). All simplifications were demonstrated in Figures 2.3 and 2.4.

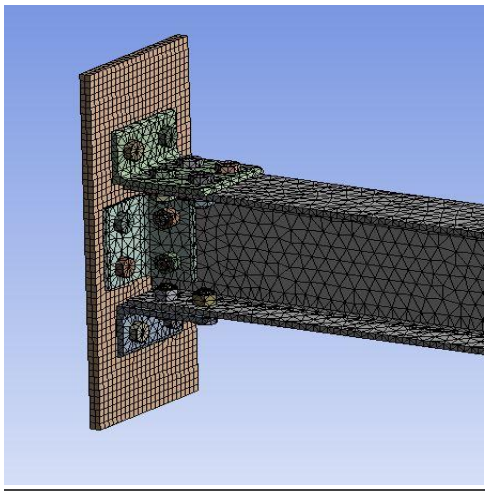

Figure 2. 3 3-D Finite Element Partially-Restrained Connection Models

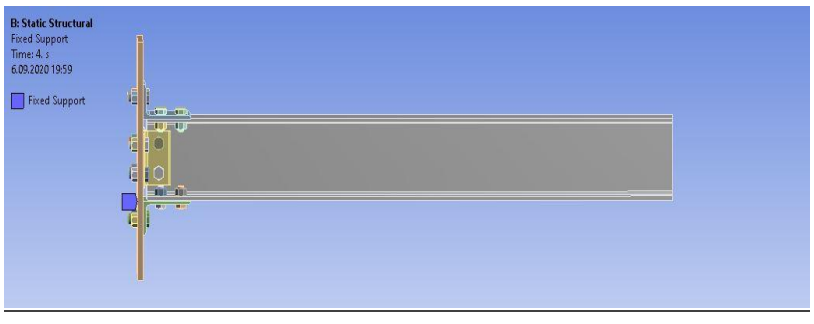

Figure 2. 4 Model Representation with Fixed Support and Column Flange

2.3. Material Properties

Material properties for finite element modeling are extremely important in which members of connection must be conveniently simulated, such as beam, column flanges, and angles or bolts and nuts. Azizinamini (Azizinamini, 1985) specified ASTM A36 mild carbon steel for whole connection members in test specimens. Mechanical properties for supplied material that was selected from test specimens are presented in Table 2.2. However, the temperature effect on the material property was not mentioned by the researcher in the experimental work. Therefore, a typical stress-strain curve has been adopted for mild carbon steel in this thesis and is demonstrated in Figure 2.5.

Table 2. 2 Presented Mechanical Properties of ASTM A36 in the Azizinamini's Experimental Research (Source: (Azizinamini, 1985))

Designation	**Mechanical Properties Ksi (Mpa)**		
	Yield Stress ksi (Mpa)	**Ultimate Strength ksi (Mpa)**	**Elongation in 2-inch Gage Length (percent)**
A36	42.8 (295)	69.9 (482)	23.8
	42.9 (295.7)	67.9 (468)	22.9
	39.3 (271)	68 (469)	32.5
	37.6 (259)	69.9 (482)	31.9
	36.5 (251)	71.9 (496)	31.3
	43.7 (301)	69.9 (482)	31.3
	40 (276)	64 (441)	34.4
	38 (262)	66 (455)	37.5

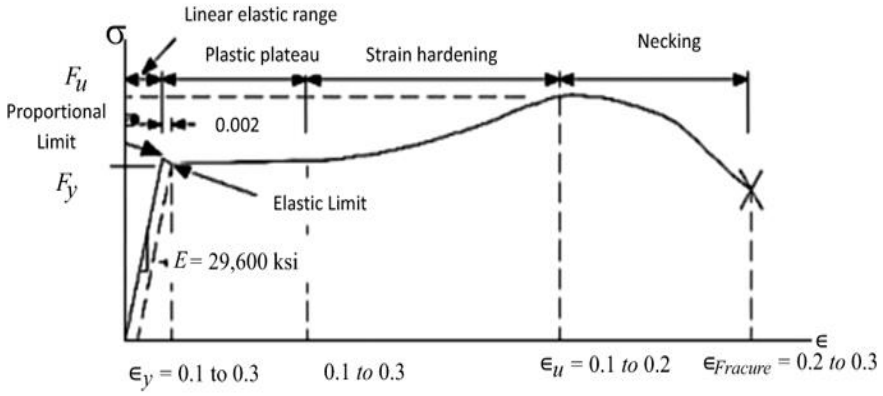

Figure 2. 5 A Typical Stress–Strain Diagram for Mild-Carbon Steel

The stress-strain diagram demands function for providing continuity in FE analysis. However, a bilinear expression should be considered to facilitate material modeling without substantial changes in member response as used in prior researches (Pirmoz & Danesh, 2009; Danesh, Pirmoz, & Daryan, 2006; Fakih, Chin, & Doh, 2018). Therefore, in the combination of the stress-strain diagram and Azizinamini's test results, a bilinear isotropic hardening model was composed for the definition of 3-D stress-strain relation in ANSYS. In this process, needed material values, which were specified to flatten out the curve, are shown as follows in Table 2.3.

Table 2. 3 Used Properties of A36 Steel Material

Modulus of elasticity, E-steel = 30000 ksi (207000 Mpa)
Yield stress of A36 steel, F-yield = 40 ksi (276 Mpa)
Ultimate Stress of A36 steel F-ultimate = 70 ksi (483 Mpa)
Tangent Modulus of A36 steel Et = 182 ksi (1255 Mpa)

The beam-column connections for all specimens were made using either 3/4-inch (19.05 mm) diameter or 7/8-inch (22.23 mm) diameter ASTM A325 heavy hex high-strength bolts with compatible ASTM A325 nuts. Bolt holes were specified as standard size that is 1/16 in (1.5875 mm) greater than bolt shank diameter for both bolt diameters. Azizinamini (Azizinamini, 1985) described the tightening method of bolts and nuts and the characteristic behavior of that connection components in the research. There is no

information about mechanical, physical properties, and pretension values of bolts and nuts in detail. Therefore, Specification for Structural Joints Using ASTM A325 or A490 Bolts (ASTM A325 & A490, 2004) approved by the research council on structural connection is used with previous researches to complete the missing information in the bolt and nut modeling process. In the light of specification and literature, information on the mechanical properties of bolts is presented below.

Specification	Material	Nominal Size Range inc (mm)	Mechanical Properties	
			Yield Strength Min ksi (Mpa)	Tensile Strength Min ksi (Mpa)
ASTM A325 TYPE 1	Medium Carbon Steel, Quenched and tempered	1/2-1 (12.7mm-25.4mm)	92 (634)	120 (827)
		1-1-1/2 (25.4mm - 38mm)	81 (558)	105 (724)

Figure 2. 6 ASTM A325 Mechanical properties

(Source: (ASTM A325 & A490, 2004))

Table 2. 4 Used Properties of A325 Bolt Material

Modulus of elasticity, E-steel = 30000 ksi (207000 Mpa)
Yield stress of Bolts, F-yield = 92 ksi (634 Mpa)
Ultimate Stress of Bolts F-ultimate = 120 ksi (827 Mpa)
Tangent Modulus of Bolts Et = 558 ksi (3847 Mpa)

2.4. Faying Surface Friction and Bolt Pretension

Basic parameters for FE analysis in ANSYS are bolt pretension and friction. Because of the clamping between the connecting components given by bolt pretensions, the forces are transmitted through friction. No information is figured out on the conducted pretension values during the experimental research.

Moreover, the faying surfaces' state is unclear. Azizinamini (Azizinamini, 1985) said that the bolts should be tightened using an air wrench utilizing the turn-of-the-nut method, with the pretension value equal to their proof load. Thus, common design values from specifications and previous researches are utilized for the analysis.

Table 2. 5 Minimum Bolt Pretension According to ASTM A325 and A490 Specification (Source: (ASTM A325 & A490, 2004))

Nominal Bolt Diameter db in (mm)	Specified Minimum Bolt Pretension, kips (KN)	
	ASTM A325 Bolts	ASTM A490 Bolts
1/2 (12.7)	12 (53.378)	15 (66.723)
5/8 (15.875)	19 (84.516)	24 (106.757)
3/4 (19.05)	28 (124.55)	35 (155.687)
7/8 (22.225)	39 (173.48)	49 (217.962)
1 (25.4)	51 (226.86)	64 (284.686)
1-1/8 (28.575)	56 (249.1)	80 (355.857)
1-1/4 (31.75)	71 (315.82)	102 (453.718)
1-3/8 (34.925)	85 (378)	121 (538.234)
1-1/2 (38.1)	103 (458.166)	148 (658.336)

Table 2. 6 Specified Values for Bolt Pretension

For the ASTM A325 3/4 in. bolts	$F_{pretension}$= 30 kips (133.446 KN)
For the ASTM A325 7/8 in. bolts	$F_{pretension}$ = 39 kips (173.480 KN)

Specified pretension values are aimed to represent the real effect of pretension force on connection response in FE analysis. Pretension forces have also influenced faying surfaces by clamping force to produce friction forces between members. Therefore, these forces take an important role in the connection behavior, especially for transferring load and its efficiency.

One of the most important factors affecting the connection's slip and moment rotation behavior is the friction value. A model was consisted of Azizinamini’s

(Azizinamini, 1985) specimens to investigate the effect of different friction coefficient values on a moment-rotation curve under constant pretension force (Citipitioglu, Haj-Ali, & White, 2002).

In this thesis, previous researches and specification classifications were considered to specify faying friction coefficient as an appropriate constant value in the modeling process. This value was chosen as 0.35 in the convenient condition of class A according to AISC (AISC 360-16, 2016; Citipitioglu, Haj-Ali, & White, 2002) as follows:

Class A: On blast-cleaned steel surfaces, this class denotes unpainted, mill scale, or surfaces with Class A coatings. For this class, the mean friction coefficient is equal to 0.35.

Class B: Surfaces having class B coatings or unpainted blast-cleaned steel surfaces fall into this category. The mean friction coefficient is equal to 0.5 for this class.

2.5. Application with ANSYS Workbench

Mechanical problems generally contain static and/or dynamic structural analyses that are linear or nonlinear, heat transfer and flow problems, as well as acoustic and electromagnetic problems. For the solution of these problems, ANSYS should be used to simulate the interaction of all disciplines of physics in these areas. This simulation opportunity through advanced computer technology allows products to be tested in a virtual environment before they are produced. In addition, as a result of simulations in the virtual environment, it is possible to detect and improve the weak points of the structures for possible problems.

The object or structure to be analyzed in this comprehensive software is divided into a finite number of smaller elements, and the selected unit element is a geometric shape. The purpose of this is that it is easy for us to analyze and solve small elements whose geometric structure is known. Decreasing the unit element size provides a more precise solution. However, increasing the number of equations enhances the processing time. Stress, displacement, temperature, etc., is obtained at the end of the analysis from the element nodes and the average of these data belonging to the node points gives information about structural components. Thus, the characteristic feature of components or structures is formed from these finite elements containing defined geometrical and mechanical data.

In this thesis, finite element analysis using ANSYS is performed in five definition stages as follows

- Material properties of structural components (i.e., stress-strain relations),
- Chosen Element Types,
- Describing contact surfaces in connection region,
- Meshing for bolts, nuts, and structural members,
- Assign supports and loads.

- *Material Properties*

The Engineering Data module of ANSYS Workbench provides stress-strain relations for steel material. Nonlinear material parameters were simplified with mechanical features defined before by using some hardening model that is available in the program as follows

Table 2. 7 Mechanical Features of ANSYS Workbench

Bilinear isotropic hardening
Multilinear isotropic hardening
Bilinear kinematic hardening
Multilinear kinematic hardening

For material properties of the components in the connection, such as beam, angles, bolts, and nuts, are composed through the ‘Bilinear Isotropic Hardening Model’ as demonstrated in Figures 2.7 and 2.8.

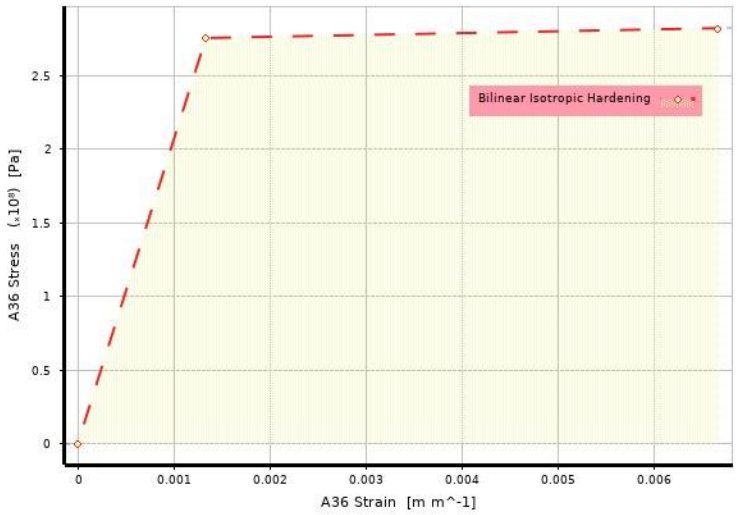

Figure 2. 7 Defined Stress-Strain Relation of A36 Steel Material in ANSYS Engineering Data Module.

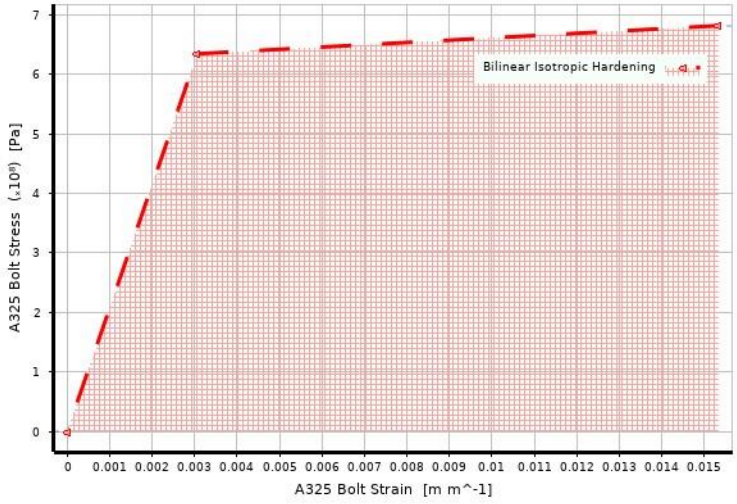

Figure 2. 8 Defined Stress-Strain Relation of A325 Steel Material in ANSYS Engineering Data Module.

- *Chosen Element Types in the Software*

An element is the basic building block of finite element analysis. In general, there are several basic types of elements that are used depending on the type of object that is to be modeled for finite element analysis and the type of analysis that is going to be performed. An element is a mathematical relation that defines how the degrees of freedom of a node are related to the next. These elements can be lines (trusses or beams), areas

(2-D or 3-D plates and membranes), or solids (bricks or tetrahedral). And also, the elements, of course, can be of higher order, which simply means they have more nodes than those we defined.

SOLID187 element is a higher-order 3-D, 10-node element, as seen in Figure 2.9. SOLID187 has a quadratic displacement behavior and is well suited to modeling irregular meshes. The element is defined by ten nodes having three degrees of freedom at each node: translations in the nodal x, y, and z directions. The element has plasticity, hyper-elasticity, creep, stress stiffening, large deflection, and large strain capabilities. It also has mixed formulation capability for simulating deformations of nearly incompressible elastoplastic materials and fully incompressible hyper-elastic materials (Akgönen & Güneş, 2017; Johnson, 2001; ANSYS INC., 2015).

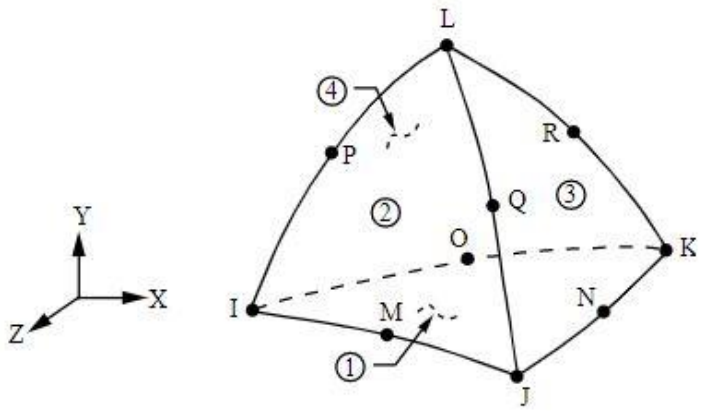

Figure 2. 9 Geometry of SOLID187

(Source: (Akgönen & Güneş, 2017))

The SOLID187 element type is the most suitable characteristic type for semi-rigid connections in nonlinear 3D finite element analysis.

Contact surfaces are also important to define the connection areas between the elements. Surface elements are located on the surfaces of 3-D solid with mid-side nodes, and it has the same geometric characteristics as the solid. This interaction of contact surfaces is composed between beam and angles, angles and column flange, bolt shank, and bolt hole. Bolts can be assumed to be clamped to fastener parts, i.e., bolt to nut. Thus, bolt and nut are kept with enough strength from moving by the clamping forces. Apart

from these clamped forces, friction forces and the slip must be recognized by the simulated interactions. Such characteristics have a significant influence on the reaction of a patterned connection.

CONTA174 element represents contact and, deformable and sliding surfaces are defined between 3-D target surfaces. This element can be applied to the connection analysis of 3D structures and joined areas. Contact takes place when the element surface penetrates an associated target surface. The element also allows the separation of bonded contact to simulate interface delamination. This is needed during the loading process for the slip state.

TARGE170 is used to represent various 3-D "target" surfaces for the related contact elements (CONTA173, CONTA174, CONTA175, CONTA176). The contact elements themselves overlap the solid, shell, or line elements describing the boundary of a deformable body and are potentially in contact with the target surface, defined by TARGE170. On the target segment element, any translational or rotational displacement, temperature, forces, and moments can be imposed.

Pretension force is also described with another element type in the ANSYS Workbench module. PRETS179 is used to define a 2-D or 3-D pretension section within a meshed structure. The PRETS179 element has solely one translation degree of freedom that represents the defined pretension direction. The software transforms the geometry of the problem so that, internally, the pretension force is applied in the specified pretension load direction, regardless of how the model is defined (Akgönen & Güneş, 2017; Johnson, 2001; ANSYS INC., 2015).

- *Describing contact surfaces in the connection region*

Contact analysis is a naturally non-linear process and the definition of surface interaction. Therefore, it is also one of the most important aspects of semi-rigid relation modeling by using sophisticated 3-D finite element software. Each contact body can be individually and carefully modeled to represent actual physical behavior in simulations with adequate precision. There are different nonlinear types of contact choice in the program, and they are briefly explained below

Bonded: No penetration, separation, or sliding between faces or edges. This is the default contact type in the software.

No Separation: Similar to bonded, except frictionless sliding can occur along contacting faces.

Frictionless: No penetration allowed, but surfaces are free to slide and separate without resistance.

Rough: Similar to the frictionless setting except no sliding allowed (i.e., friction coefficient=infinite).

Frictional: Allows sliding with resistance proportional to the user-defined coefficient of friction; free to separate without resistance.

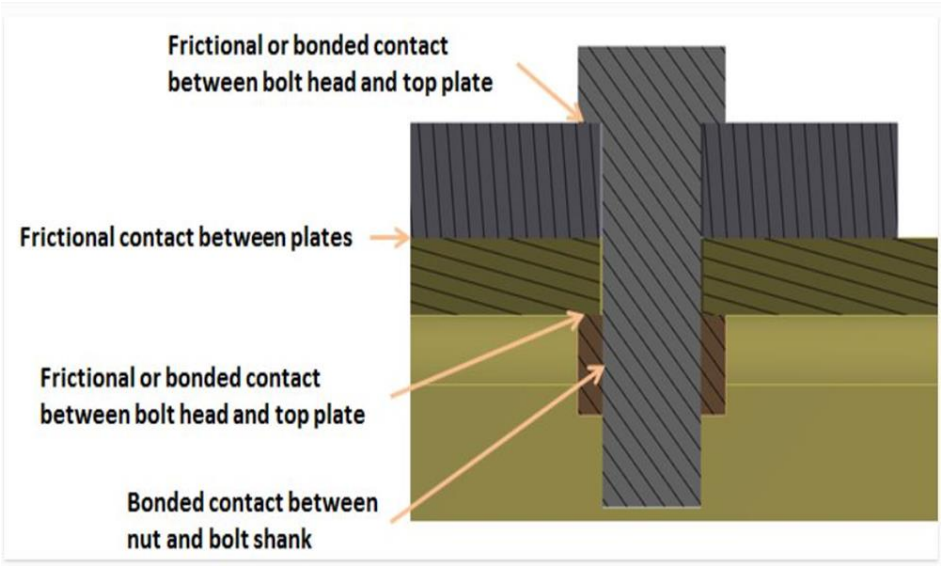

Figure 2. 10 Illustration of Appropriate Contact Types on Bolt, Nut, and Plate Surfaces

The form of contact to be used in a semi-rigid steel connection should be frictional since there is always friction between contact surfaces. Convenient selection of contact surfaces is a critical task in the modeling process because this step is come up with a convergence problem that should be observed at even early modeling stage when contact tool is used to check. For the pretension force in the bolts, the selection of frictional contact between bolt and nut surfaces is more realistic but is not necessary and does not provide further accuracy in results. Therefore, in this thesis, frictional contact among plates, bolt-plate surfaces, and bonded contact between bolt-nut surfaces were chosen. Contact selections and appropriate options between surfaces are displayed in Figure 2.10.

- *Meshing for bolts, nuts, and structural members*

Meshing is an integral part of the engineering simulation process where complex geometries are divided into simple elements that can be used as discrete local approximations of the larger domain. The mesh influences the accuracy, convergence, and speed of the simulation. Furthermore, since meshing typically consumes a significant portion of the time it takes to get simulation results, the better and more automated the meshing tools, the faster and more accurate the solution. Therefore, when the modeling process comes to the meshing step, the user should manage the process easily with minor interventions offered by the program. There are four types of meshing options that are significantly influencing the user for analysis quality and time duration:

- Method,
- Sizing,
- Contact Sizing,
- Refinement.

Mesh methods are roughly divided into two groups, 2D and 3D. These are the triangle and the quadrilateral for 2D and tetrahedron, quadrilateral pyramid, triangular prism, and hexahedron for 3D cell shapes. The default meshing method is a tetrahedron, and in this study default meshing property was chosen. These commonly used cell shapes illustrations are presented below

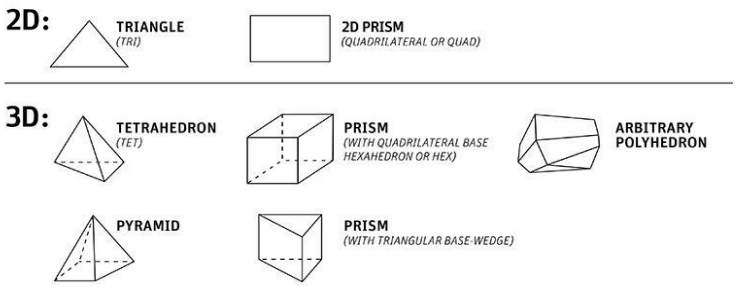

Figure 2. 11 Basic 2D and 3D Cell Shapes

The size of the mesh may also be set in different ways with the option of "sizing" in ANSYS. Relevant center module very important option for setting the meshing. The user should choose from coarse / medium / fine choices. These options have the automatic meshing sizing provided by the program, and the default mode is coarse. The sizing option is demonstrated in detail in Figure 2.12 with decided points for meshing 8S2.

Sizing	
Use Advanced Si...	Off
Relevance Center	Coarse
Element Size	11.430 mm
Initial Size Seed	Active Assembly
Smoothing	Medium
Transition	Fast
Span Angle Center	Coarse
Minimum Edge L...	9.16540 mm

Figure 2. 12 Meshing Element Size for 8S2 Specimen

Contact sizing and refinement property in the meshing procedure should be used to increase analysis accuracy and handle convergence issues for body parts at contact surfaces, especially where robust nonlinearities take place. However, very fine mesh results in excessively long durations of analysis and the processing of vast volumes of data. Therefore, these mesh options should be assessed in load transfer regions between discrete body surfaces such as I-beam and L-shape angles, angles, and column flanges.

In the study, to find ideal meshing, from coarser to finer meshing steps was performed and discovered that analysis was affected by very coarse mesh causing error for stress distribution in contact region members. On the other hand, the I section beam was not affected extremely to transfer the load to the angles.

In the meshing result, to model the semi-rigid connection properly, the connection region between the column flange and beam end requires detailed meshing. Since the connection region is composed of top-bottom and web angles that connect the beam to the column has a strong nonlinear response. Therefore, these parts meshed fine. Conversely, the I-section beam solely transfers the loads acting at the free end to the connection region. Thus a coarse mesh was chosen along the length of the beam.

If mesh quality is also desired after its modeling is completed, the ‘Mesh Metric’ option allows one to view metric information and thereby evaluate the mesh quality. Once

the mesh model has been generated, view information can be chosen about any of the following mesh metrics: Element Quality, aspect ratio for triangles or quadrilaterals, jacobian ratio, skewness. These are the most preferred. Element quality and aspect ratio options were used here to briefly explain the mesh quality of the model.

Element quality factor is computed for each element of a model, and it provides a composite quality metric that ranges between 0 to 1. This metric is based on the ratio of the volume to the edge length for a given element. A value of 1 indicates a perfect cube or square, while a value of 0 indicates that the element has a zero or negative volume (ANSYS INC., 2015).

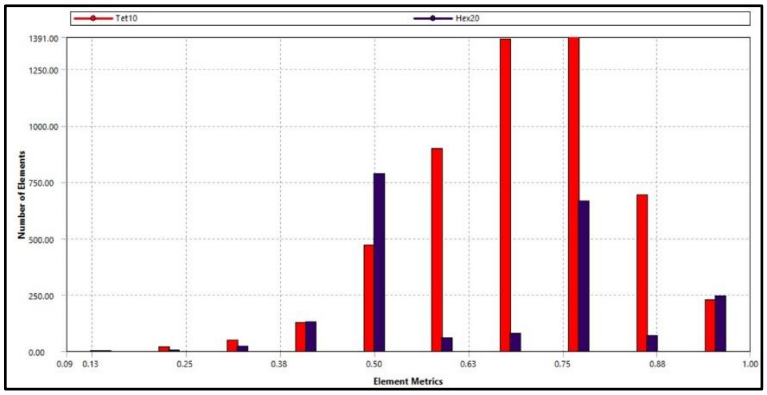

Figure 2. 13 Element Quality of Mesh Metric for the 8S10 Connection Model in ANSYS

As seen in Figure 2.13, the mesh quality of the connection based on ‘Element Quality’ is 0.70 on average. And connection components that are top-seat and double web angles are between 0.75 and 0.88.

The aspect ratio for a triangle or quadrilaterals is computed in the following manner, using only the corner nodes of the element. The best possible triangle aspect ratio for an equilateral triangle is 1. A triangle having an aspect ratio of 20 is shown in Figure 2.14. And also, the best possible quadrilateral aspect ratio for a square is one. A quadrilateral having an aspect ratio of 20 is shown in Figure 2.14 (ANSYS INC., 2015).

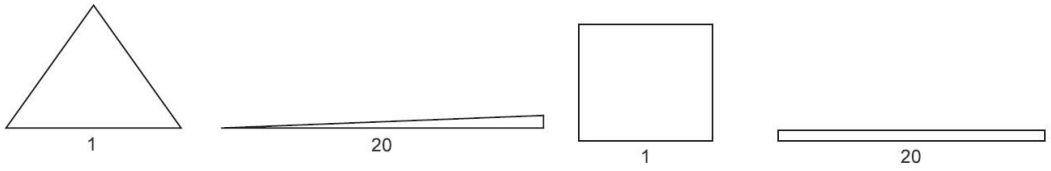

Figure 2. 14 Aspect Ratio Calculations for Triangles and Quadrilaterals

(Source: (ANSYS INC., 2015))

As seen in Figure 2.15, the mesh quality of the connection based on the ‘Aspect Ratio’ is two on average. And connection components that contain top-seat and double web angles are around 1.5.

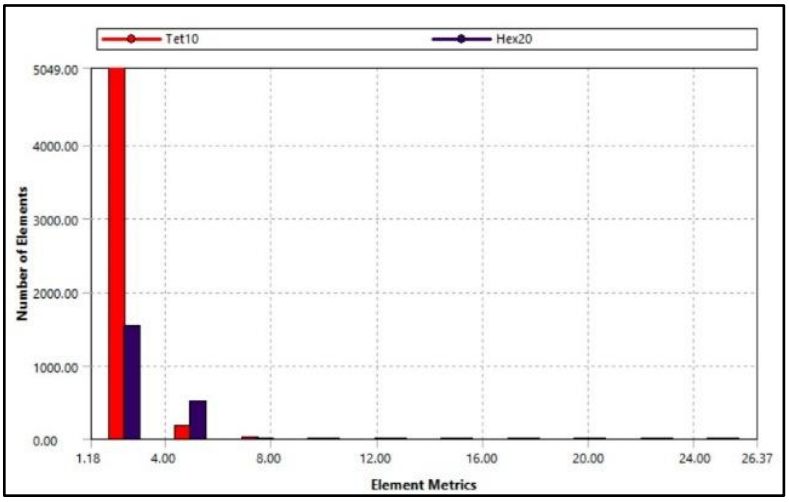

Figure 2. 15 Aspect Ratio of Mesh Metric for the 8S10 Connection Model in ANSYS

Several iterations were conducted to find an appropriate mesh model for enough mesh quality without convergence problems. Then, as explained above, the most convenient mesh model applied to the connection models was expressed through element quality and aspect ratio approaches.

- *Assign Supports and loads*

As previously stated, just the column flange is modeled, assuming that it is an adequately rigid component due to the column stiffeners. Therefore, fixed support was assigned to the backside of the column flange. The force was applied as displacement by selecting meshed nodes at the beam end to prevent convergence problems with the purpose that is not exceeding plastic strain capacity in meshing for the chosen element type.

A proper definition of bolt pretension is needed to define an accurate nonlinear behavior of semi-rigid connections. Bolt pretension allows shear forces operating on the bolt to be transferred without damaging the hole region, and connection stiffness is improved prior to loading. Bolt pretension loading is demonstrated below.

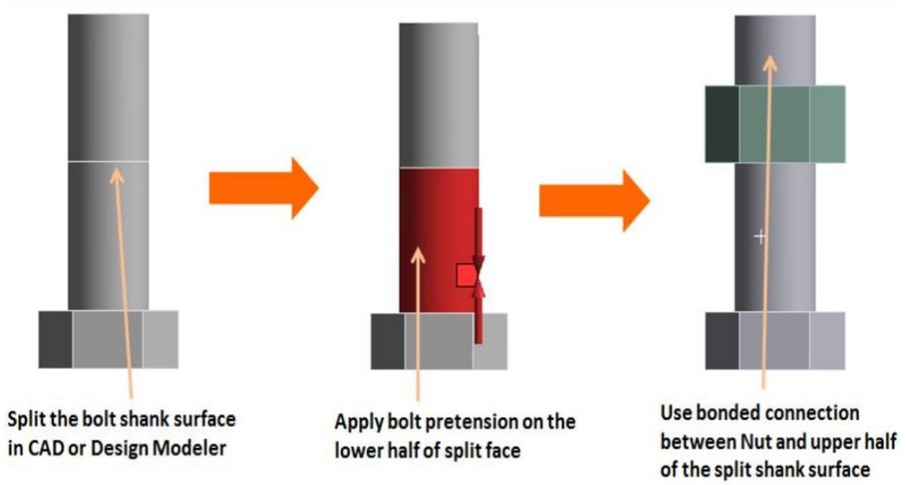

Figure 2. 16 Application of Bolt Pretension Force

In ANSYS Workbench, loading conditions are separated into sub-loadings concerning time steps when pretension force is to be applied. The first time step or steps represents pretension forces, and then the external displacement is following in related time steps. Carrying out pretension force on the bolt shank in ANSYS Workbench, the bolt shank must be divided from the face at which bolt and nut have in contact. This process should be completed through cad programs or the ANSYS design modeler. After splitting the bolt shank, pretension force is assigned to the lower face of the bolt shank,

and bonded contact is defined to the upper surface of the split shank and nut. All loading representation and fixed support boundary conditions are illustrated in Figure 2.16.

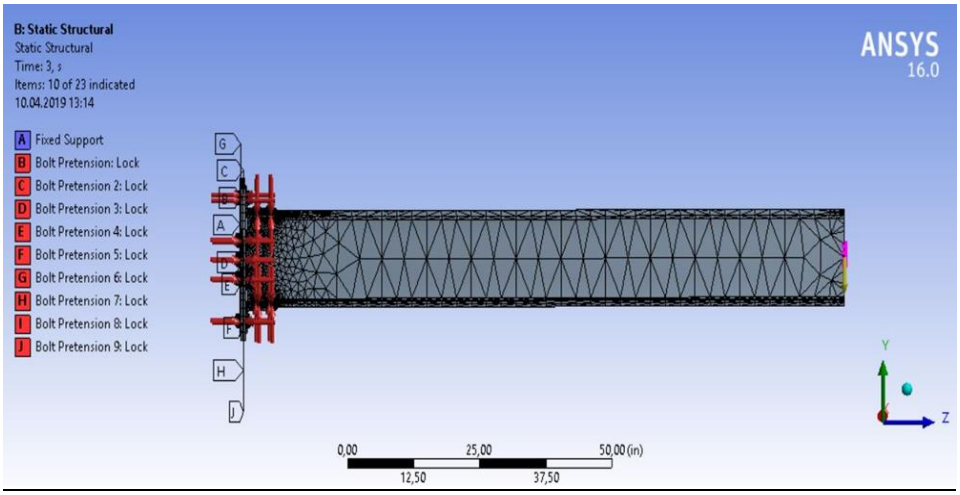

Figure 2. 17 Representation of External Displacement and Pretension Forces with Fixed Support

All web nodes of the beam were restrained against out-of-plane displacement to prevent the structure as well as to restrain the beam against lateral-torsional buckling. Beam sections used in connection models were compact, which eliminated the possibility of instabilities due to local buckling following Azizinamini's experimental work. Hence, buckling failure modes were ignored in the current FE investigation. To obtain moment-rotation curves to compare experimental study, the force-displacement response of the connection is converted by using simple equations 2.1 and 2.2, as shown below

$$M = P_d.L \tag{2.1}$$

$$R = \frac{\varepsilon_1 - \varepsilon_2}{h_d} \tag{2.2}$$

Where M is applied connection moment, P_d is the summation of the reactions of applied displacement on beam end nodes; L corresponds to beam length, R is the relative rotation of connection, h_d is beam depth, ε_1 and ε_2 are relatively top and bottom flange horizontal displacements.

2.6. Finite Element Modeling Results

In this chapter finite element modeling procedure is described in detail to create a practical and applicable semi-rigid connection model with support from experimental data. When researchers intend to get more detail from the test setups for finite element modeling and analysis process, they easily discover some missing information in Azizinamini's (Azizinamini, 1985) thesis to convert the work to the computer environment. In this point, literature search, specifications, and codes helped for making up these deficiencies. Not only missing information completed with these documents but also boundary conditions are specified to facilitate the modeling process by preserving analysis quality without any serious errors in the results. All this collected knowledge is interpreted and used within the relevant parts of finite element analysis. For the representation of relevant Azizinamini test specimens, eleven distinct finite element models have been created. Azizinamini's 14S1 research demonstrates the expected deformed shape of the connection region, i.e., the column face connecting to the beam by angles and bolts.

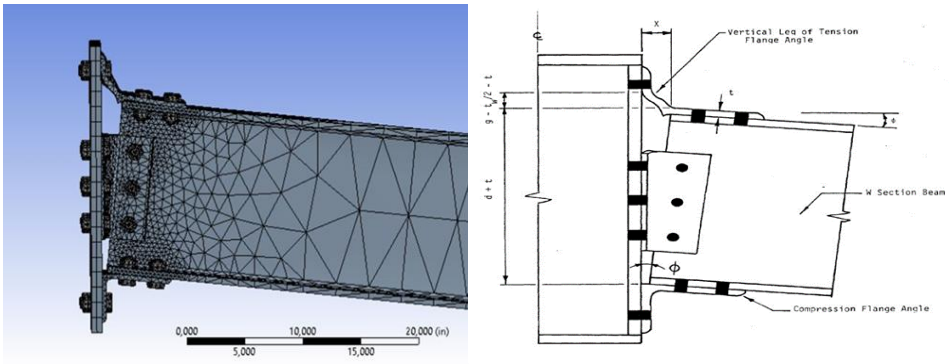

Figure 2. 18 Schematic Representation of the 14S1 FE Model with Expected Deformed Shape

(Source: (Azizinamini, 1985))

The first verification of the FE modeled specimens is the observation of a good physical match between the deformed shape of the finite element model and the deformed shape of the experimental model. In this case, the finite element software was able to simulate the behavior of the connection region. As seen in Figure 2.18, the top angle is

supposed to bend significantly due to the downward displacement of the beam and a void open there, and it is supposed that the bottom angle profile is compressed. Thus, the finite element modeling process was defined, and the expected behavior of the modeling result was taken place. 8S1-S2-S3-S8-S9-S10 specimens that were previously listed in Table 2.1 will be discussed with experimental and mathematical results on moment-rotation curves at the end of chapter 3. The task of this section was to make detailed modeling in the finite element environment based on the TSADWA connection with the experimental data and to ensure the compatibility of these models with the experimental deformation behavior while obtaining moment-rotation curves.

CHAPTER 3

MATHEMATICAL MODEL FOR SEMI-RIGID CONNECTION

Several analytical models have been developed to represent semi-rigid connection behavior. Previous models used the initial stiffness of the connection as the key parameter in a linear M- θ model. Although the linear model is very easy to use, it has a serious disadvantage. It is not suitable for a full range of rotation. A closer approximation of true connection behavior can be obtained by using either bilinear or piecewise linear models. Bilinear approach for calculating the moment-rotation curve of semi-rigid frames was used in many computer programs. However, it should be noted that modeling of joint behavior with linear or bilinear element methods allows for limited sensitivity since the moment-rotation behavior of steel beam to column connection is nonlinear even at low load levels. Therefore, if sensitive representation is desired, a nonlinear connection model should be chosen. Figure 3.1 demonstrates a summary of past attempts to represent connection behavior in a mathematical form, the M-θ relationship of beam-to-column connection.

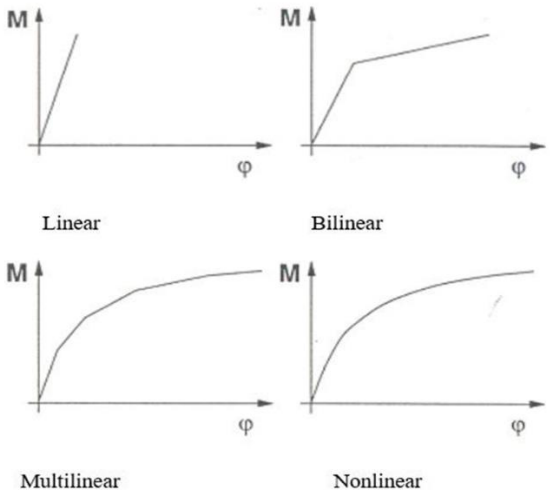

Figure 3. 1 Different Mathematical Expressions of the Moment-Rotation Curve

(Source: (Faella, Piluso, & Rizzano, 1999))

3.1. Linear model

This is the simplest connection model, with only one parameter describing a connection's stiffness. The initial stiffness of connections can be easily determined by tests, and it remains constant throughout the study without the need to update it. In the early phases of creating semi-rigid connection analysis tools, the linear semi-rigid connection model was frequently employed. When deformations exceed the linear range, as seen in Figure 3.2, this model fails. In vibration and bifurcation analysis, this model is recommended and most commonly employed (Chan & Chui, 2000; Faella, Piluso, & Rizzano, 1999).

3.2. Multi-linear model

When the linear range of response is exceeded, the multi-Linear model was developed to better represent the nonlinear behavior of connections. In order to improve the accuracy of the analysis, multi-linear models have been presented. The bi-linear and multi-linear models both outperform the linear model, as seen in Figure 3.2. They may, however, have discontinuities in slope, resulting in divergence and complexity in numerical analysis, making the creation of more continuous functions for moment-rotation relations necessary (Chan & Chui, 2000; Faella, Piluso, & Rizzano, 1999).

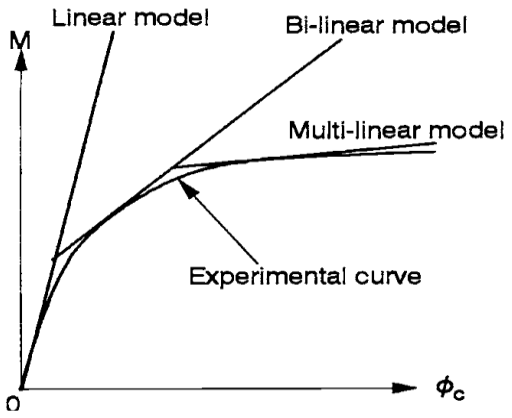

Figure 3. 2 Comparison of Linear, Bilinear Multilinear Models

(Source: (Chen & Lui, 1991))

The relationships of semi-rigid connections with mathematical expressions can be divided into two categories to describe moment rotation curves. The first category is generated by such mathematical representations based on one or more parameters with an obvious physical meaning and a shape function. These depictions can be referred to as stiffness, strength, and shape factor-based formulations. On the other hand, the second category can be referred to as curve fitting formulations since the parameters do not have any obvious physical meaning as they derive particularly from a regression analysis. While the first group is called an analytical mathematical model, the second group is called an empirical mathematical model for predicting moment rotation curves.

Empirical models are based on the use of empirical formulas related to the geometrical and mechanical properties of the beam to column connections of the parameters involved in the mathematical representation of the moment-rotation curve. These empirical formulations can be derived by regression analysis. In this thesis, Frye and Morris's (Frye & Morris, 1975) polynomial curve fitting mathematical model was adopted due to its easy implementation and convenient standardization parameters for TSADWA connection.

3.3. Polynomial curve fitting model

Curve-fitting the experimental data with the simple iterative procedure is an extensively used approach to explain the M-θ curve of flexible connections. Therefore, the experimental moment-rotation curve is exclusively approximated to a polynomial type function using curve fitting techniques. Sommer, in 1967, first fitted moment-rotation data to standardized moment-rotation curves within the style of non-dimensional polynomial series. This work was applied to header plate connections. The form of the polynomial series function is

$$\theta = f(KM) \tag{3.1}$$

Where K is a factor to allow for the size effects or dimensions of the connection, the standardized moment-rotation function applies to all connections of the same type.

Frye and Morris (Frye & Morris 1975) expanded on Sommer's work on standardized moment-rotation curves by proposing an odd-power polynomial function based on Sommer's technique (1969). It has the form as

$$\varphi = C1(KM)^{1} + C2(KM)^{3} + C3(KM)^{5} \quad (3.2)$$

Where K is the standardization parameter that depends on geometrical properties and connection type, C1, C2, and C3 values are the curve fitting constants obtained from the experimental data.

Frye and Morris used the method of least squares to determine the constants of the polynomial. The primary disadvantage of this model is that the first derivative of this function which indicates connection stiffness may be discontinuous and/or possibly negative, which is physically impossible (Chan & Chui, 2000; Chen & Kishi, 1989). Although it has the problem, curve fitting polynomial model was performed by many researchers due to its simplicity (Şeker, Doğan, & Kozanoğlu, 2017; Jones, Kirby, & Nethercot, 1983; Sagiroglu & Aydin, 2015; Hayalioglu, Degertekin, & Görgün, 2004).

Frye and Morris's assumptions and limitations show adaptation with performed finite element analysis and Azizinamini's experimental semi-rigid connection tests. These assumptions for simplification are mentioned as follows

- The effects of shear and axial load on connection deformation are neglected,
- All members are prismatic and straight,
- Possible buckling of individual members or portions of the structure is disregarded,
- The effects of strain hardening are ignored,
- Except for the nonlinear force-deformation properties of the connections, the system behaves linearly.

In the light of considering these assumptions, connection standardization parameters and geometric properties are listed in table 3.1 and demonstrated in figure 3.3 for each related connection type.

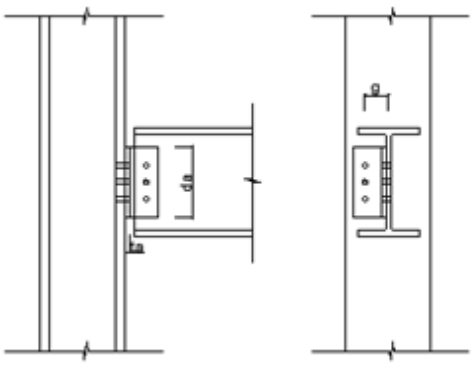

Single Web Angle

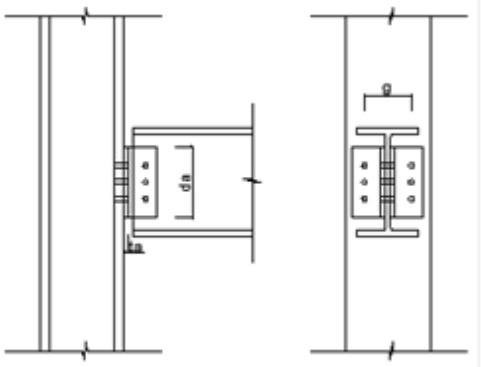

Double Web Angle

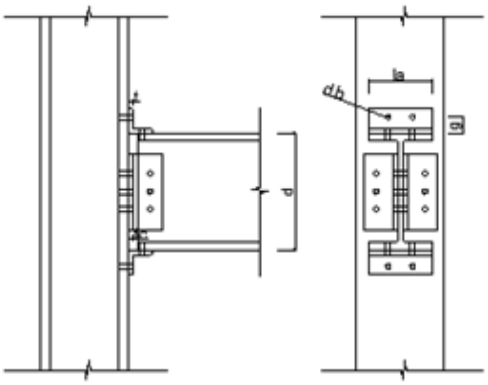

Top and Seat Double web angle

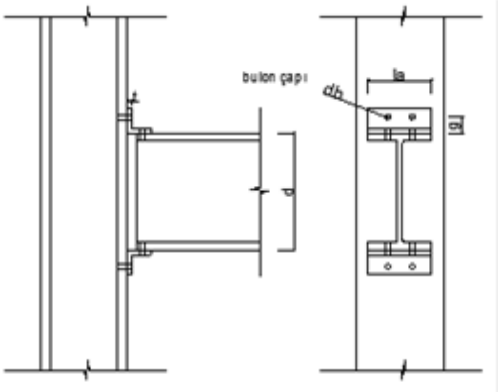

Top and Seat Angle

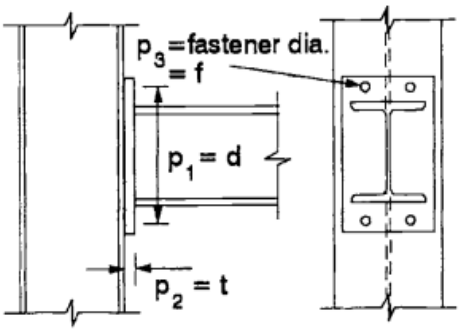

Endplate No Column Stiffener

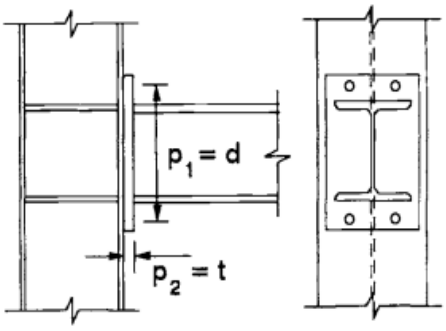

Endplate with Column Stiffener

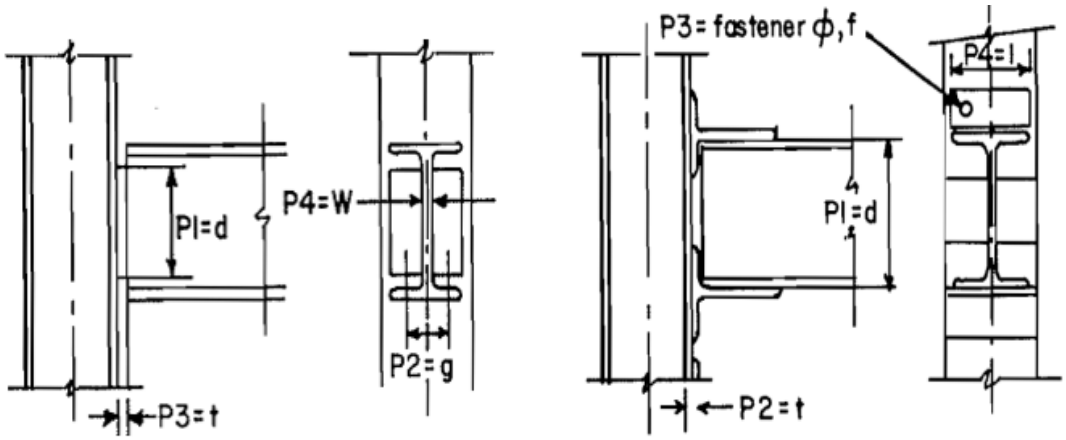

Header Plate T-Stub

Figure 3. 3 Connection Types and Standardization Parameters for the Frye and Morris Polynomial Model.

(Source: (Frye & Morris, 1975))

Frye and Morris's mathematical model was composed of the most commonly used structural steel framing connection types that have been stated in a standardized, non-dimensional form. The regression analysis approach and TSADWA connection type give enough accuracy due to a large number of connected data to fit the curve. Therefore, by creating a successful iterative procedure with these documents, it is possible to represent the non-linear partially restraint top-seat and double web connection behavior of the structure in a practical way. There is insufficient knowledge and sample data on the accomplished semi-rigid connection type; the linear and multi-linear models are skipped.

Table 3. 1 Standardization and Curve-Fitting Constants (Source: (Chan & Chui, 2000; Frye & Morris, 1975; Prabha, et al., 2015))

Connection types	Curve fitting constants	Standardization constants
Single web-angle connection	$c_1 = 4.28 \times 10^{-3}$ $c_2 = 1.45 \times 10^{-9}$ $c_3 = 1.51 \times 10^{-16}$	$\kappa = d_a^{-2.4} t_a^{-1.81} g^{0.15}$
Double web-angle connection	$c_1 = 3.66 \times 10^{-4}$ $c_2 = 1.15 \times 10^{-6}$ $c_3 = 4.57 \times 10^{-8}$	$\kappa = d_a^{-2.4} t_a^{-1.81} g^{0.15}$
Top and seat angle with web-angles connection	$c_1 = 2.23 \times 10^{-5}$ $c_2 = 1.85 \times 10^{-8}$ $c_3 = 3.19 \times 10^{-12}$	$\kappa = d^{-1.287} t^{-1.128} t_c^{-0.415}$ $l_a^{-0.694} g^{1.35}$
Top and seat angle without web-angles connection	$c_1 = 8.46 \times 10^{-4}$ $c_2 = 1.01 \times 10^{-4}$ $c_3 = 1.24 \times 10^{-8}$	$\kappa = d^{-1.5} t^{-0.5} l_a^{-0.7} d_b^{-1.5}$
End plate without column stiffeners connection	$c_1 = 1.83 \times 10^{-3}$ $c_2 = 1.04 \times 10^{-4}$ $c_3 = 6.38 \times 10^{-6}$	$\kappa = d_g^{-2.4} t_p^{-0.4} d_b^{-1.5}$
End plate with column stiffeners connection	$c_1 = 1.79 \times 10^{-3}$ $c_2 = 1.76 \times 10^{-4}$ $c_3 = 2.04 \times 10^{-4}$	$\kappa = d_g^{-2.4} t_p^{-0.6}$
T-stub connection	$c_1 = 2.10 \times 10^{-4}$ $c_2 = 6.20 \times 10^{-6}$ $c_3 = -7.60 \times 10^{-9}$	$\kappa = d^{-1.5} t^{-0.5} l_t^{-0.7} d_b^{-1.1}$
Header plate connection	$c_1 = 5.10 \times 10^{-5}$ $c_2 = 6.20 \times 10^{-10}$ $c_3 = 2.40 \times 10^{-13}$	$\kappa = d_p^{-2.3} t_p^{-1.6} t_w^{-0.5} g^{1.6}$

Where db, t, b, d, tc, g is the diameter of bolts, the thickness of angles, flange width of the beam, depth of beam web, flange thickness of column, and gauge distance, respectively. All section parameters are used in inches.

3.4. The Result of TSADWA Connection Models

In the previous chapter, top-seat and double web angle semi-rigid connection is modeled and analyzed through the ANSYS Workbench software by explaining the process that contains simplifications and its suitability for Azizinamini's experimental research. And now, the curve-fitting mathematical model was adopted to obtain the

moment-rotation curve practically for taking nonlinear partially restraint connection effect into analysis results. However, the mathematical model should be used with caution before taking to its time-saving advantage since different variables or uncertainties in the connection region can show themselves as the error on moment-rotation curves. Therefore, comparison of finite element analysis and experimental specimens with the mathematical model gain significance since uncertainties that the connection has can be determined individually. Firstly, the comparison of finite element analysis and its experimental study specifies boundary conditions to handle the convergence issues, and If the iterative lines are closely related to each other, finite element modeling and experimental study demonstrate convenience. Then, simplified mathematical models should be obtained for these curves and practically used in frame design, especially for performance optimization. In the light of this perspective, a triple comparison of models is presented by converting the unit system in SI for all of them, as shown in Figures 3.4 to 3.9.

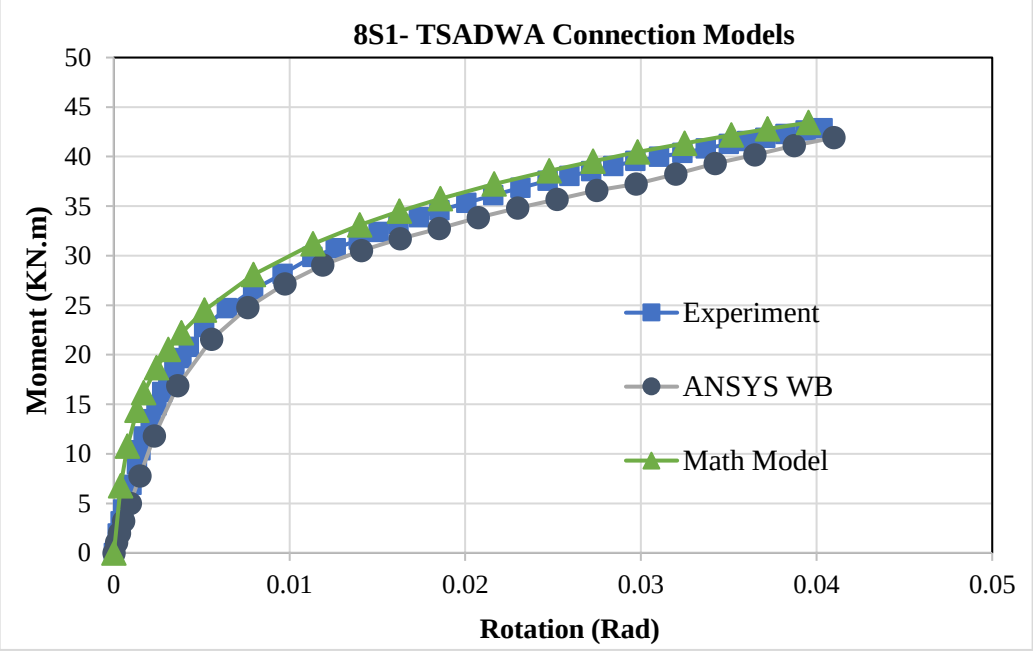

Figure 3. 4 Comparison of Finite Element Analysis and Curve-Fitting Polynomial Mathematical Model with the 8S1 Experimental Result.

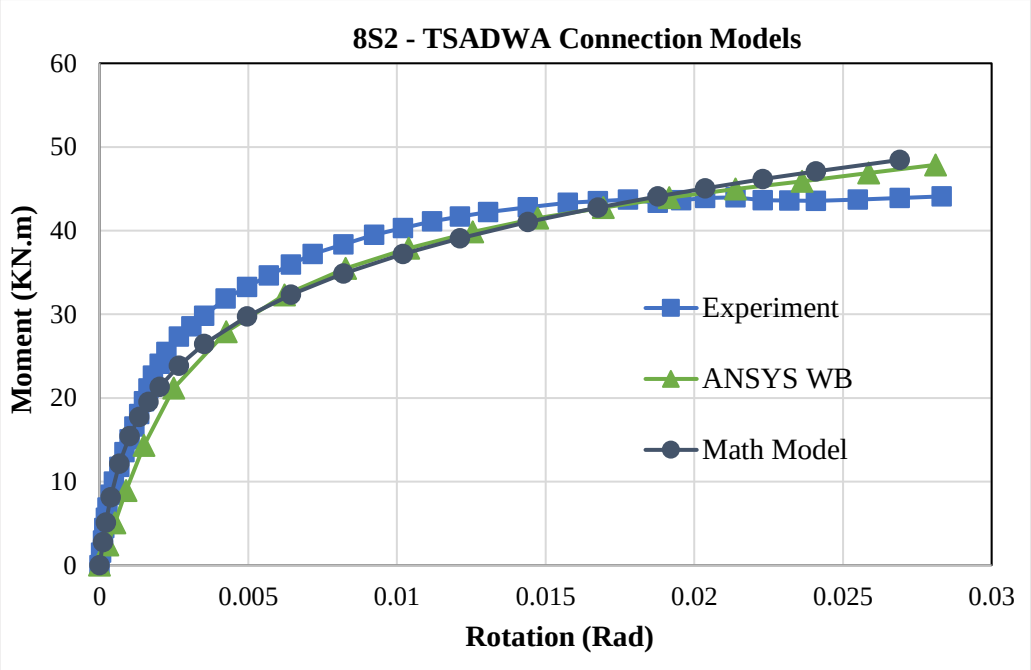

Figure 3. 5 Comparison of Finite Element Analysis and Curve-Fitting Polynomial Mathematical Model with the 8S2 Experimental Result.

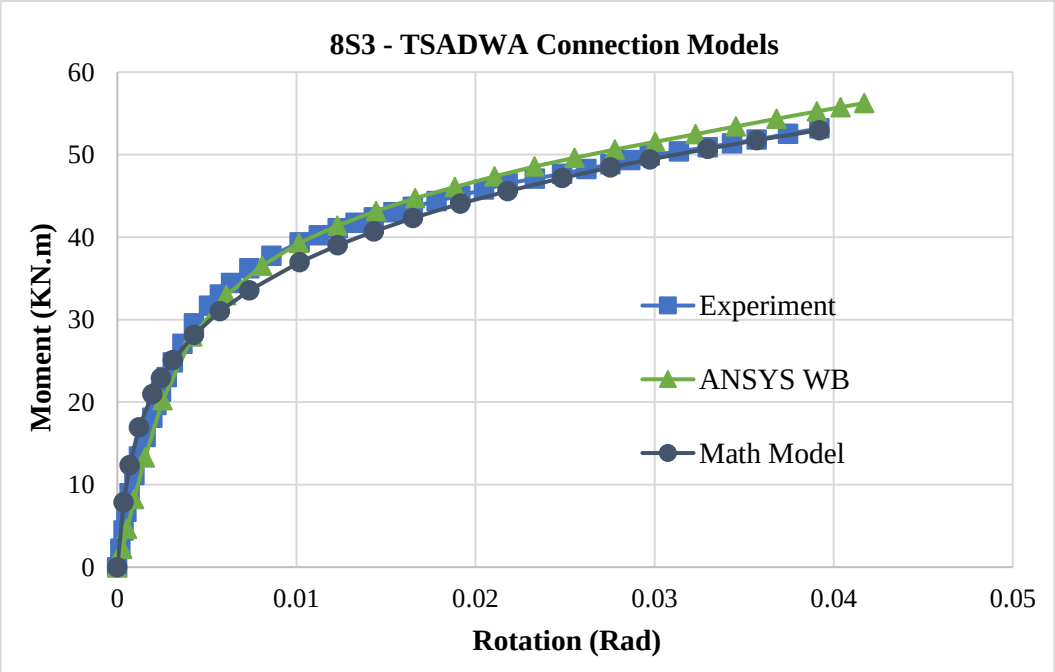

Figure 3. 6 Comparison of Finite Element Analysis and Curve-Fitting Polynomial Mathematical Model with the 8S3 Experimental Result.

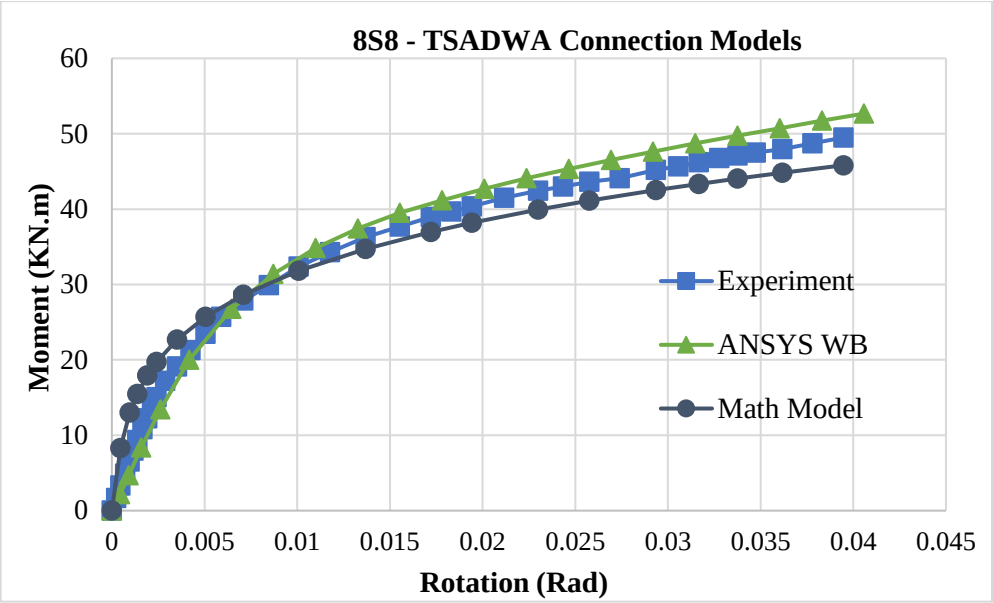

Figure 3. 7 Comparison of Finite Element Analysis and Curve-Fitting Polynomial Mathematical Model with the 8S8 Experimental Result.

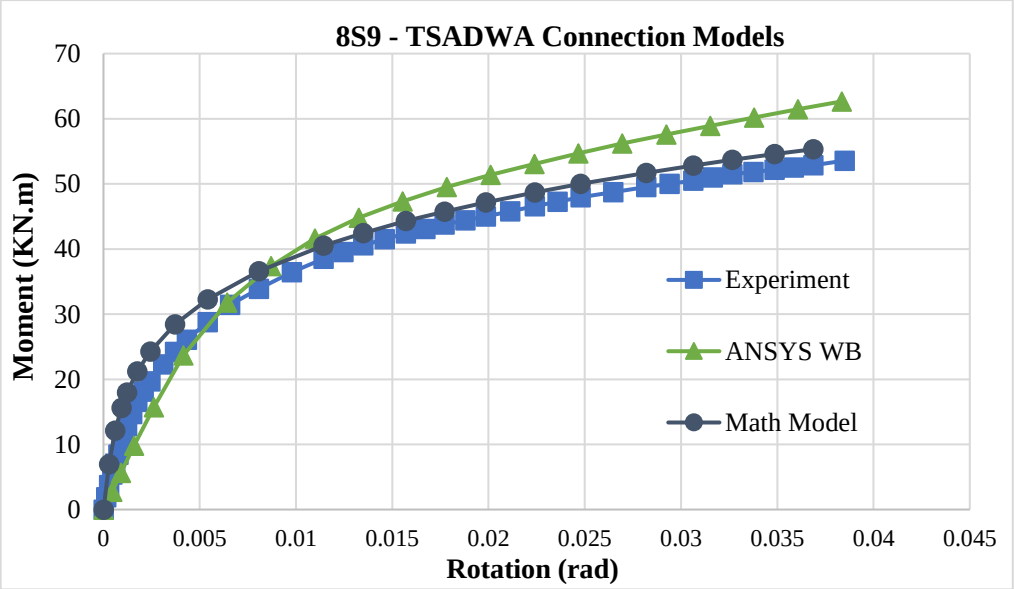

Figure 3. 8 Comparison of Finite Element Analysis and Curve-Fitting Polynomial Mathematical Model with the 8S9 Experimental Result.

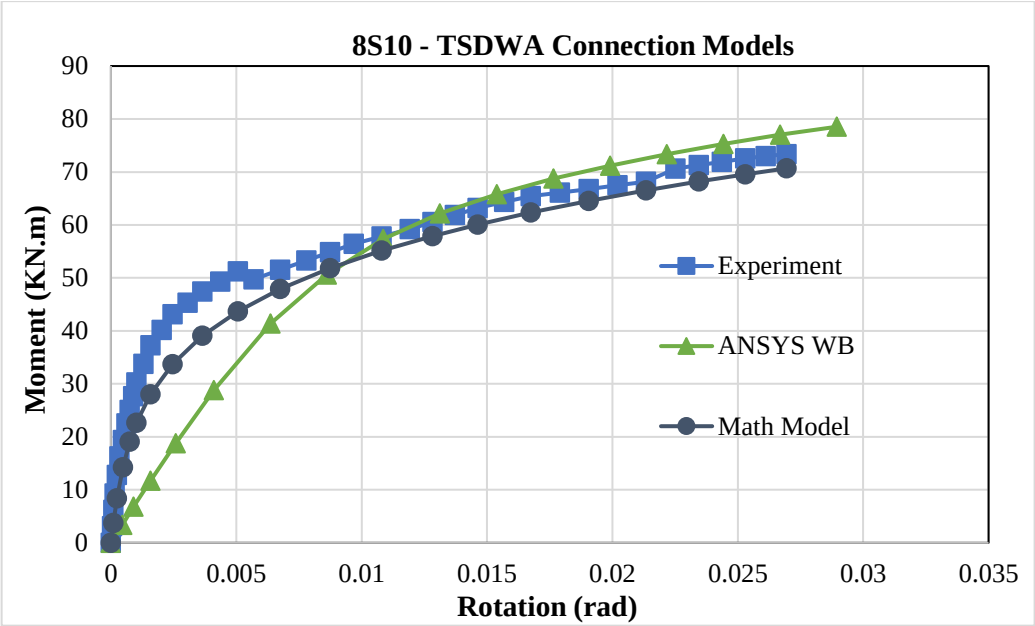

Figure 3. 9 Comparison of Finite Element Analysis and Curve-Fitting Polynomial Mathematical Model with the 8S10 Experimental Result.

As a general result of to present study through the moment rotation curves, the mathematical and FE models are close enough to the experimental TSADWA moment-rotation diagram to use for the connection or frame design. In a test sample and process, there are various uncertainties. Moreover, even at the same steel material, its yield strength may change, and differences in the modulus of elasticity and residual stresses are widespread in steel members (Citipitioglu, Haj-Ali, & White, 2002; Pirmoz & Danesh, 2009). Therefore, some errors and divergence issues on the analysis results in comparison to experimental results can be observed consciously where they come from.

Despite errors in secondary stiffness in some curves, the nonlinear response from the connection's finite element analysis follows the same tangent as the experimental response. This thesis seeks to demonstrate the moment-rotation performance of a semi-rigid connection via the top and seat angle with a double web angle connection using 3-D nonlinear finite element analysis. The compatibility of the mathematical model with the obtained moment-rotation results reveals that semi-rigid connections can be modeled in the finite element environment and can be confirmed by mathematical models without the need for experimental data. In this study, comparisons of these models also provide insight for structural engineers to comprehend the capability of nonlinear behavior of semi-rigid connections. This study shows that the non-linear behavior of semi-rigid connections in practical design applications is a complex operation. However, with

powerful computer technology and developed appropriate mathematical models, enough accuracy and practical usage should be provided on connection behavior for the design process.

TSADWA connection model results were examined due to its actual semi-rigid connection behavior. Azizinamini's experimental study (Azizinamini, 1985) was used to compare with Frye and Morris mathematical (Frye & Morris, 1975) and 3D finite element models. The purpose of these chapters was to investigate close enough for the connection member's behavior and moment-rotation capacities of different section variables. During the process, getting less time consumption for the analysis with economic results without needed experimental outcomes was also aimed. In the continuation of the thesis process, the effect of semi-rigid connections on the structural frame will be examined, and a comparison of PR and FR connections in the frame models will be present.

CHAPTER 4

PUSH-OVER ANALYSIS OF RIGID AND (TSADWA) SEMI-RIGID STEEL MOMENT FRAMES

In recent decades, the majority of steel structure design has centered on the application of the linear analytic technique. Although an elastic analysis can demonstrate a structure's elastic capacity and show where the initial yielding would occur, it cannot anticipate failure mechanisms or account for force redistribution. Engineers are seeking to better understand how structures respond when significant earthquakes occur and where the elastic capacity of structures is exceeded by using inelastic approaches for design and evaluation.

Under a strong earthquake, structures undergo considerable inelastic deformation, and dynamic structural characteristics alter with time. Nonlinear analytical procedures contribute to understanding the actual behavior of structures by specifying failure modes and the potential for progressive collapse. Inelastic analysis methods are separated basically into two categories which are known as nonlinear dynamic (Time History) analysis and nonlinear static (Push-Over) analysis. Although nonlinear dynamic analysis assures a more realistic and reliable result of seismic performance, the method needs several earthquake excitation records to be used to obtain desired target limits on a structure. This demands more time and effort in comparison to nonlinear static analysis. The capacity of nonlinear static analysis to represent transient dynamic behavior with cyclic loading and degradation is restricted. However, the nonlinear static procedure gives convenient and adequately reliable results in single-mode dominated structures, that dynamic response is also governed by first-mode sway motion. Due to its easy implementation and practical usage, nonlinear static pushover analysis was adopted in this study.

4.1. Definition of Pushover Analysis

Examination of nonlinear static analysis is based on the assumption that the response of the structure can be related to the response of an equivalent single-degree-of-freedom (SDOF) system. This implies that the response is controlled by a single mode and the shape of this mode maintains constant through the response. Although both assumptions are inaccurate, studies have demonstrated that these assumptions can meet expectations for the seismic response of multi-degree-of-freedom structures that are governed by the fundamental mode (National Institute of Standards and Technology, 2017).

The building's nonlinear analytical model is subjected to progressively increasing lateral forces until it reaches a predefined goal displacement. The most common approach to plot the force-displacement curve is by following the base shear and the roof displacement. The displacement of the roof is measured as the maximum displacement that the building would undergo during an earthquake and can be determined using any formula that allows for the effects of nonlinear activity on the building's displacement. For each loading stage, the lateral loads are added incrementally, stiffness characteristics of the building materials are renewed. The consequence of pushover analysis is the measurement of the demands of force and deformation on the building at the target displacement, and this target displacement implies the top displacement when the building is subjected to design-level ground excitation through the response spectra. Also, connections have a major effect on the frame's behavior, and their modeling is the critical point for the analysis. For semi-rigid connections, it was important to know the moment-rotation curve, to observe the yielding parameters, and to orient the pushover analysis.
Definition of push-over analysis can be briefly explained in three fundamental steps to perform practically with acceptable results,

- Geometric nonlinearity with loading condition,
- Mechanical nonlinearity with plastic hinge definition,
- Limit Conditions (BCs) of the frame with code specification.

- *Application of Loads*

Gravity loads are applied gradually in the studies to represent the current condition of the connections before the application of lateral loads. In addition to gravity loads, any other distributed or point load can be implemented to the structure due to taking the P- Δ effect into consideration. For starting pushover analysis, lateral load based on the first mode is assigned to the structure according to the distribution of inertia forces imposed on the structure.

- *Material Behavior of Steel Elements and Components*

The modeling of yielding characteristics of column and beam members are determined by the FEMA-356 (FEMA-356, 2000) standard, as shown in Figure 4.1.

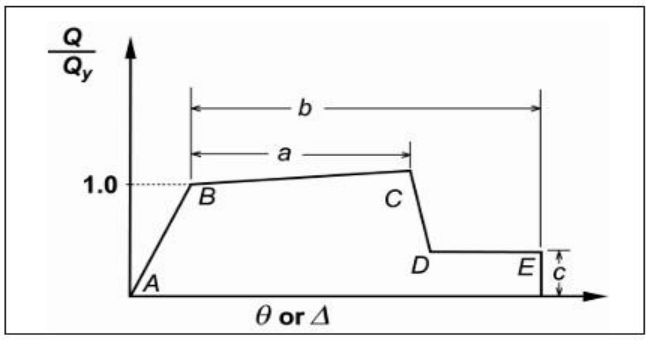

Figure 4. 1 FEMA-356 Generalized Force-Deformation Relation for Steel Elements or Components

(Source: ((FEMA-356, 2000))

Based on FEMA-356 (FEMA-356, 2000) definitions, Figure 4.1 can be expressed as the following:

- The linear response is represented by the line segment connecting point A (unloaded component) and point B (effective yield).

- The strain hardening model response of the materials can be derived from points B to C. For beams and columns, a strain-hardening slope of 3% of the elastic slope is allowed unless testing results justify a higher strain-hardening slope.
- It is the ordinate peak value for the whole curve, and Point C may be used to determine the component's strength. It's also worth noting that after Point C, the component loses a substantial amount of strength.
- Between Points D and E, the component continues to lose strength beyond Point C.
- The component has essentially zero strength after Point E.

FEMA-356 (FEMA-356, 2000) considers an essential aspect when modeling components based on that curve: When utilized as modeling input in nonlinear computerized analytic software, the abrupt shift from Point C to Point D may create computational issues and inability to converge. To avoid this computational instability, the portion of these curves between points C and D is given a small slope.

- *Limitations of Pushover Analysis*

Estimating target displacement, selecting lateral load patterns, and recognizing failure processes are critical circumstances that influence the precision of pushover outcomes. There are many methods to provide critical circumstances related to the desired performance level of building for capacity curves. These methods should be referred ATC-40 (ATC-40, 1996) or FEMA-356 (FEMA-356, 2000). In this thesis, FEMA-356 performance levels are adopted to specify the limitations of nonlinear static analysis for capacity and push-over curves. Different performance levels according to FEMA-356 (FEMA-356, 2000) are described as follows:

Structural Performance Level S-1, Immediate Occupancy, means the post-earthquake damage state in which only very limited structural damage has occurred. The basic vertical- and lateral-force-resisting systems of the building retain nearly all of pre-earthquake strength and stiffness. The risk of life-threatening injury as a result of structural damage is very low, and although some minor structural repairs may be appropriate, these would generally not be required before re-occupancy.

Structural Performance Level S-2, Damage Control, is defined as the range of damage states between the Life Safety Structural Performance Level (S-3) and the Immediate Occupancy Structural Performance Level (I-1) (S-1).

Structural Performance Level S-3, Life Safety refers to the post-earthquake damage state in which the structure has sustained considerable damage but still has a margin of safety against partial or total structural collapse. Although several structural elements and components have been seriously damaged, there has been no significant risk of falling debris, either within or outside the structure. Although injuries may occur as a result of structural damage, the overall risk of life-threatening damage is predicted to be minimal. The building should be repairable; nevertheless, for economic reasons, this may not be feasible. While the damaged structure is not in danger of collapsing, structural repairs or temporary bracing should be installed before re-occupancy.

Structural Performance Range S-4, Limited Safety, shall be defined as the continuous range of damage states between the Life Safety Structural Performance Level (S-3) and the Collapse Prevention Structural Performance Level (S-5).

Structural Performance Level S-5, The post-earthquake damage situation in which a structure is on the edge of partial or total collapse, is referred to as collapse prevention. Major structural damage has occurred, potentially resulting in significant loss of the lateral-force resisting system's stiffness and strength, large permanent lateral deformation of the structure, and to a smaller extent, loss of vertical-load-carrying capacity. All important components of the gravity load-resisting system, on the other hand, must continue to carry their gravity load demands. There is a significant danger of damage from falling structural debris. The structure may not be repairable and is not safe for re-occupation since aftershock activity might cause it to collapse.

In this thesis, Life Safety Performance Level (S-3) is taken as a reference for the target displacement value. As mentioned in FEMA-356 (FEMA-356, 2000) following the Life Safety Performance Level (S-3), top drift was limited up to 2.5% for steel moment frames, and primary structural components have damage as local buckling of some beam elements and severe joint distortion; isolated moment connection fractures, but shear connections remain intact. A few elements may experience partial fracture (FEMA-356, 2000). In the light of this information, pushover analysis is continued until reaching target displacement value or consisting hinge in one of the base story columns.

When connections were faced with greater moments than their ultimate moment resistance capacity, the stiffness of this connection was taken as zero in the next load step.

This implies that there is no further rotation resistance in the connection. It does, however, maintain its part in providing to the axial capacity of the beam concerned.

4.2. The Procedure of Pushover Analysis

Pushover analysis may be conducted as either force-controlled or displacement-controlled, based on the actual design of the load and the predicted actions of the structure. The force-controlled choice is useful when the load is known, such as gravity or live load. On the other hand, the displacement-controlled method should be used where defined drifts are needed, such as seismic loading. The displacement-controlled pushover study is generally divided into the following steps (FEMA-356, 2000; ATC-40, 1996):

- Bilinear or trilinear load-deformation graphs which influence the lateral response are described.
- Vertical loads consisting of dead loads and live loads were added to the structural model as initial loading.
- Assign lateral load pattern by considering the first mode shape of the structure to the selection of loading node.
- Displacements are enhanced until some member(s) yield under the combination of gravity and lateral loads.
- Base shear and roof displacement are reported at first yield.
- The stiffness of yielded member(s) is reduced to revise the structural model.
- Apply a new lateral displacement increment to the updated structure in order for another element (or group of elements) to yield. It's worth noting that the actual forces and rotations for elements at the start of a new increment are the same as they were at the end of the preceding one. Each application of a lateral load increment, on the other hand, is a distinct analysis with zero initial circumstances. As a result, to decide when the next element yields, add the forces from the current analysis to the sum of the prior increments' forces. Similarly, to determine element rotations, add the current analyses' rotations to the total of the preceding increments' rotations.

- Add the increment of the lateral load and the resulting rise in the displacement of the roof to the previous totals, giving the calculated values of the base shear and the displacement of the roof.
- Repeat the last three steps until the structure reaches an ultimate limit (structural instability); distortions considerably beyond the target performance level.

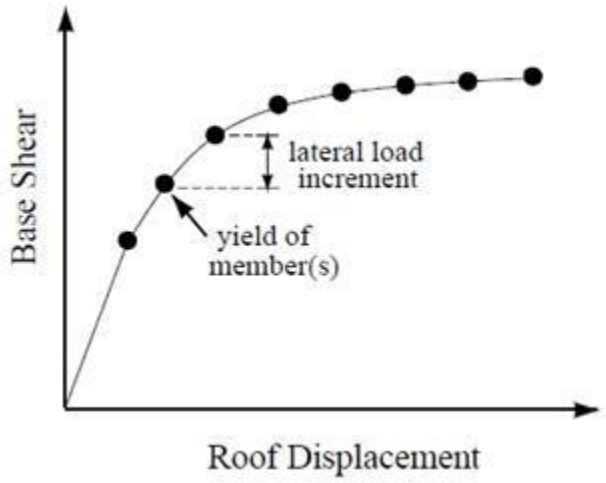

Figure 4. 2 Capacity (Push-over) Curve of Structure

(Source: (ATC-40, 1996))

4.3. Modeling of Push-Over Analysis for Frames with SAP2000

As is well known, pushover analysis, like other methods of analysis in the literature, has its own set of assumptions for modeling structural member reaction. Nonlinear force-deformation properties of the beam and column members for a frame are the key assumptions in the pushover analysis from that perspective. Various software has different usage to represent nonlinearity in members for this purpose. All the pushover analyses of the frames were carried out in SAP2000.

For pushover analysis, SAP2000 provides two options: force-controlled and deformation-controlled. A specified lateral load pattern is administered in a progressively rising way in force-controlled pushover analysis, with the research terminating automatically when the complete lateral load level is reached. The defined lateral load

pattern is applied gradually in the same way as in force-controlled pushover analysis, but the analysis is recorded at defined joint roof displacement levels, and the analysis ends when the defined roof displacement is attained in deformation-controlled pushover analysis. The deformation-controlled pushover analysis is most commonly used in practice. This option is particularly useful for observing the structure's large-displacement behavior and ductility level (CSI Analysis Reference Manual, 2017).

4.3.1. Nonlinear Material Behavior of Columns and Beams in SAP2000

The nonlinear force-deformation properties of the frame members (columns and beams) are specified for each member to represent yielding behavior, and the location of the hinges on the frame members is critical. In the scope of this study, all the columns and beams' yielding behavior were modeled via default hinges of SAP2000. The tips of column members were assigned the axial force-major axis bending hinges, while the tips and middle points of beam members were allocated the major axis bending hinge property. Based on SAP2000 definitions, Figure 4.3 can be explained as the following:

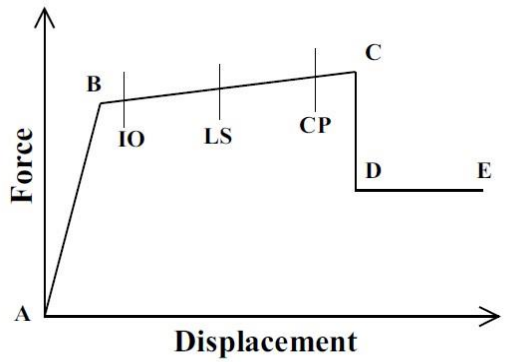

Figure 4. 3 SAP2000 Default Generalized Force-Deformation Relation for Hinge Modeling

(Source: (CSI Analysis Reference Manual, 2017))

It's worth noting that in SAP2000, hinge characteristics solely describe the hinge's plastic behavior. This means that the frame members' elastic behavior is described by the user in relevant material property frame sections. As a result, hinge assignment to frame members does not affect the members' elastic behavior.

The program ignores the parts of the hinge load-deformation curve between points A and B. The B-C-D-E part of the curve describes plastic deformation after hinge yielding occurs at Point B. Point B is used as the reference plastic deformation, which means that all plastic deformation is assessed about B. Plastic deformations in the negative direction are defined using the same reasoning as positive deformations. The strain-hardening slope is defined as the line segment between Point B and Point C.

In the hinge property description in SAP2000, if the ‘Drops to Zero' option is selected, load-bearing capacity at Point E becomes zero. If the ‘Is Extrapolated' option is chosen, load-bearing capacity is extrapolated in a roughly parallel manner to the line segment between points D and E (CSI Analysis Reference Manual, 2017).

The IO (Immediate Occupancy), LS (Life Safety), and CP (Collapse Prevention) points on the curve correspond to FEMA-356 (FEMA-356, 2000) structural performance levels to meet SAP2000's 'Acceptance Criteria' selections in Figure 4.3.

The last consideration in the modeling of column and beam members’ nonlinear behavior was the determination of the location of the hinges. Their exact location is far two times cross-section depth away from the connection location, considering their intended position as mentioned above.

4.3.2. Nonlinear Geometric Behavior of Columns and Beams in SAP2000

Gravity loads acting on the structure's deformed shape cause nonlinear geometric effects, causing internal forces in members and connections to increase. The two forms of nonlinear geometric effects are P-δ effects, which are concerned with deformations together with the members and measured relative to the member chord, and P-Δ effects, which are assessed between member ends and frequently associated with story drifts in structures. P- Δ effects are significantly more of a problem than P-δ effects in buildings subjected to earthquakes (Deierlein, Reinhorn, & Willford, 2010).

The internal force and moment demands are magnified by large lateral deflections (Δ), resulting in a reduction in effective lateral stiffness. As internal forces grow, a lower proportion of the structure's capacity is available to support lateral loads, resulting in a decrease in effective lateral strength.

The basic concepts behind the P- Δ effect are illustrated in the following example, as seen in Figure 4.4 (in the Figure large deflection symbol, Δ, represented by D). When the original arrangement is inspected, the moment at the base is written as:

$$M = FL \tag{4.1}$$

And it drops linearly to zero at the loaded end. When equilibrium is examined in the deformed configuration, the axial force P acting on the transverse tip displacement, Δ, causes an extra moment. The moment no longer changes linearly throughout the length; instead, the deflected form determines the variation by Eq. 4.2.

$$M = FL - P\Delta \tag{4.2}$$

In the deformed configuration, and only the transverse deflection is taken into account. Any change at the moment force due to a change in length of the member is neglected here (CSI Analysis Reference Manual, 2017).

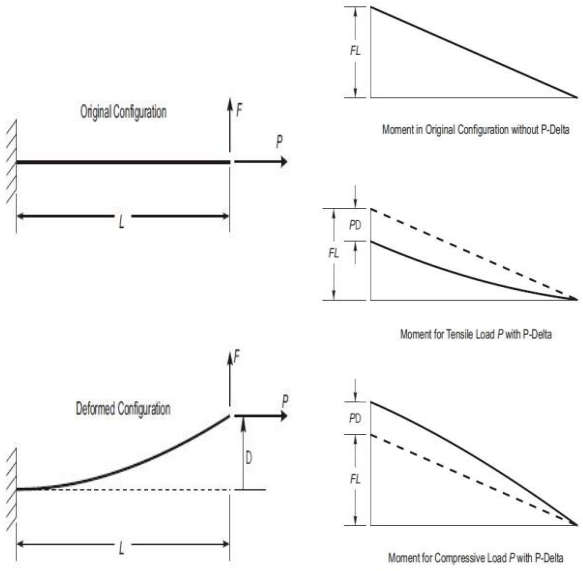

Figure 4. 4 Moment Diagrams for Cantilever Beam Examples

(Source: (CSI Analysis Reference Manual, 2017))

The moment at the base and throughout the member is reduced when the beam is in tension, the transverse bending deflection, Δ, is likewise reduced. As a result, the member is more effective in resisting the transverse load F. If the beam is in compression, the moment throughout the member increases, enhancing the transverse bending deflection, Δ. Against load F, the member is substantially more flexible.

In the light of these approaches, pushover analysis of the study was carried out in all cases by considering the effect of P-Δ with the option 'P-Delta plus Large Displacements' option of SAP2000.

4.3.3. Modeling of Nonlinear Material Behavior of Semi-Rigid Connections in SAP2000

There are two approaches to model semi-rigid connections in SAP2000. One is the same manner as the yielding of column and beam elements are modeled. By using hinges, the moment-rotation properties of semi-rigid connections can be conveniently assigned to the beam ends. The other way is modeling Link Elements to define semi-rigid connections (CSI Analysis Reference Manual, 2017). Link Elements were defined as different elements like beams and columns, and a Link Element is a two-joint connecting link. Each element is assumed to be composed of six separate "springs," one for each of six deformational degrees of freedom (axial, shear, torsion, and pure bending). Several Linear/Nonlinear link element properties give effectiveness for modeling purposes. In this study, Link Element is chosen as the 'Multi Linear Elastic' option of SAP2000. To model semi-rigid connection through Link Element, the 'Zero-Length Element' approach is adopted by a Link connecting two joints, I and j; it is permissible for the two joints to share the same location in space creating a zero-length element.

The most significant parameters of the Link Element, the directional properties, must be defined. The local coordinate system of each Link element is utilized to determine force-deformation attributes and output. This local system's axes are numbered 1, 2, and 3. The first axis relates to the extensional formation and covers the length of the element. The concept of the element local 1- 2-3 coordinate system, as well as its connection to the global X- Y-Z coordinate system, must be properly understood. Right-handed coordinate systems are used in both systems.

The first form defines directional characteristics as U1, U2, U3, R1, R2, and R3, which match to Link Elements directional features in their linked local axes. The local axes of each member are defined individually in SAP2000. The following is the definition of directions for Link Elements in the context of that study: R1: Torsional Stiffness (Global X Direction), R2: Rotational Stiffness for Minor Axis Bending (Global Z Direction), R3: Rotational Stiffness for Major Axis Bending (Global Y Direction), U1: Axial Stiffness (Global X Direction), U2: Shear Stiffness (Global Z Direction), U3: Shear Stiffness (Global Y Direction) (Global Y Direction).

On their 2-D structural models, all of the analysis and design situations were investigated. There are no torsional load demands on the members as a result. This indicates that in our research, the direction of R1 is unimportant. As a consequence, R1 was fixed in the semi-rigid connections modeling. The same approach can also be applied for the R2 direction since there is no bending load requirement in the minor axes of the frame members due to the 2-D structural analysis. Shear deformations were ignored in U2 and U3, as they were in most structural analysis situations. U2 and U3 were therefore fixed. Except for U1 and R3, other directional properties were fixed by marking the related box of the form. Considering that the connection for U1 is at least as rigid as the beam, it is deemed appropriate to fix it when the incoming force is taken into account. As previously stated, the stiffness properties in the R3 direction are the essential parameter that defines the features of the semi-rigid connection.

- *Modeling Panel Zone Behavior in SAP2000*

As illustrated in Figure 4.5, the panel zone (PZ) region, which is shared by neighboring beams and columns, is subjected to a combination of axial forces, shear forces, and moments from the connected members.

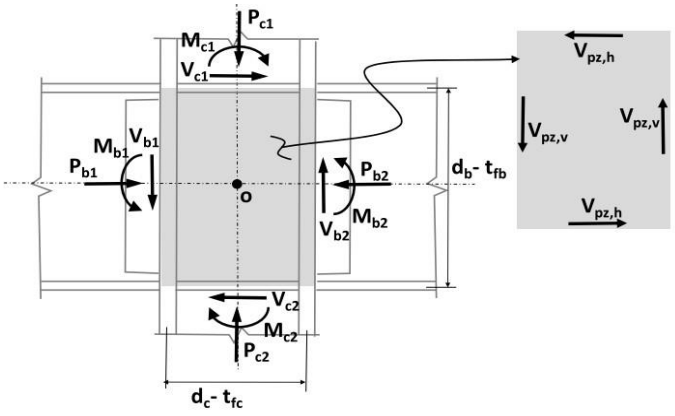

Figure 4. 5 Schematic of Forces from Beams and Columns Acting on Panel Zone and the Resultant Panel Zone Shear Forces.

(Source: (National Institute of Standards and Technology, 2017))

Modeling PZ behavior necessitates the consideration of two major factors: (1) the influence of the panel zone's limited size on the kinematics around the connection and the effective free-span lengths of the connected beams and columns; and (2) elastic and inelastic deformations in the PZ region. While it is widely accepted that the PZ shears (Vpz,h, and Vpz,v) are the most important factors affecting the PZ response, the PZ region may also be subjected to significant strains due to axial column forces, axial strains in the column flanges, and axial strains in the continuity plates caused by moments in the columns and beams (so-called "strain penetration" into the joint). In most cases, explicit modeling of all of these effects will need continuum finite element modeling (National Institute of Standards and Technology, 2017).

While such connection panels have a considerable reserve capacity beyond initial general shear yielding, the inelastic joint deformations may compromise the frame or story's strength and stability. The total frame stiffness is affected by panel-zone shear yielding, and the consequent second-order effects may be severe (AISC 360-16, 2016). Thus, for whole structural models, the PZ effect was determined by representing it through ‘Rigid Link Elements’ in SAP2000. One portal steel frame was analyzed in ANSYS FE software to figure out the stress and strain results of the PZ region. This example was performed to guarantee PZ region staying at elastic range, and then, these results are compared by ‘Rigid Link Element’ model in SAP2000 over conducted push-over analysis in ANSYS to neglect shear yielding effect in the region and on the overall frame analysis.

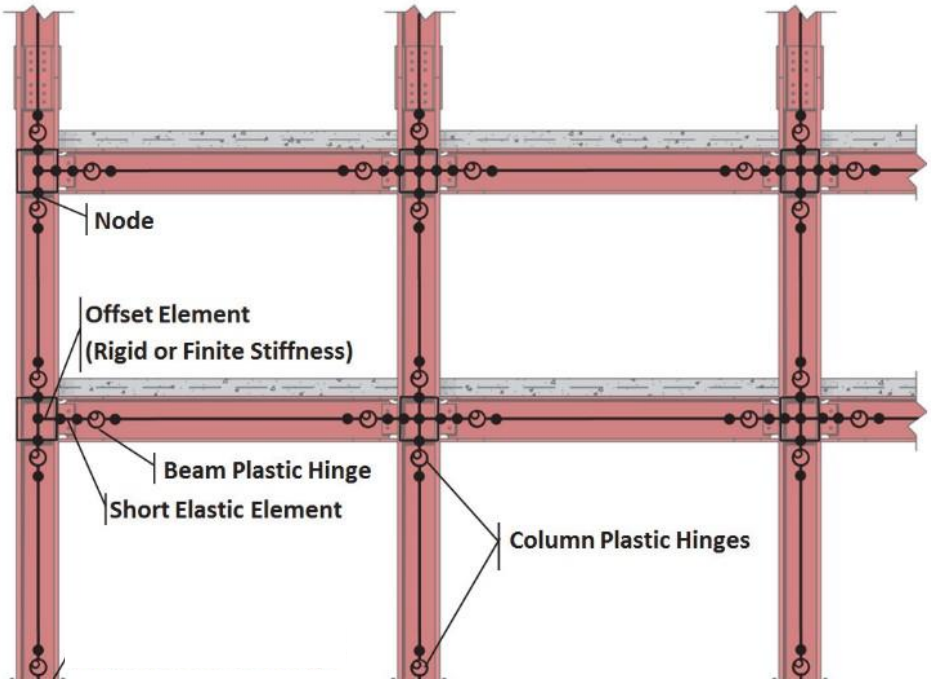

Figure 4. 6 Overview of A Typical Steel Moment Frame, Showing Concentrated Hinge Centerline Model Idealization.

(Source: (National Institute of Standards and Technology, 2017))

In the light of whole modeling assumptions and definitions mentioned above, in the study, the modeling technique was adopted according to Figure 4.6. Hinge locations and properties of beams and columns were assigned, and link elements were used to connect members' tips. 'Rigid Link Elements' for PZ region behavior and 'Multi Linear Elastic Link Element' for semi-rigid connection behavior by considering zero-link element approach is used to represent accepted modeling method.

The next section consists of examples to explain semi-rigid structural frame behavior in comparison to a rigid one. The first example was composed with a steel portal frame through ANSYS software to demonstrate the semi-rigid effect on the frame in detail and validate the approach mentioned so far. Comparing ANSYS analysis and SAP2000 analysis over push-over curves allowed interpreting of modeling approach whether it was convenient or not. Another following example is carried out by using these modeling principles and compared to which was modeled with the rigid connection of the steel frame.

4.4. Examples of Push-Over Analysis

Example 1. Semi-Rigid Steel Portal Frame

As a first example, the steel portal frame was preferred to examine ANSYS and SAP2000 frame models closely and to ensure adequate correlation of modeling approaches between them over the capacity curve.

The frame was evaluated from Azizinamini's (Azizinamini, 1985) experimental research to use known material and physical information of the connection to obtain a semi-rigid effect on the frame's capacity curve in detail. Therefore, W12x96 column section and W8x21 beam section were utilized with floor height that was selected as 144 in (3657.6 mm) and span that was specified, two times of beam span, as 133 in (3378.2 mm) due to Azizinamini's (Azizinamini, 1985) test configuration. Same material properties as in the connection analysis were assigned to the frame members and connection parts (i.e., A36 and A325). The model was modified in SPACE CLAIM software to convert the 3D solid frame to a 2D shell frame. This change was taken place so that the computational effort can be decreased to perform analysis since elements and node numbers of structural frame in 3D FE analysis didn't provide practical calculation and mostly after long-duration time analysis came up with convergence issue. During the modeling process in SPACE CLAIM share topology feature was activated to reduce contact numbers, and with this feature, contacts were only composed between semi-rigid connection (Top – seat and double web angles) surfaces. Whole contact types are used as frictional contacts with thickness effect options according to Azizinamini's (Azizinamini, 1985) semi-rigid connection study, as mentioned elaborately in Chapter 2.

The prepared frame model was kept on going with bolt connections between beam and column that are added through top – seat and web angles. 'Beam (Circular) Connection' body-to-body model was placed to the bolt holes. In this point, it should be noted that 1/16 in (1.5875 mm) greater bolt hole diameter is ignored to focus on overall frame behavior since it wouldn't be possible to use those 'Beam Connection' and 'Line Body/Joint' types in the models (ANSYS INC., 2015). In Figure 4.7, a 2D shell model can be seen through a semi-rigid connection region with the features described by now.

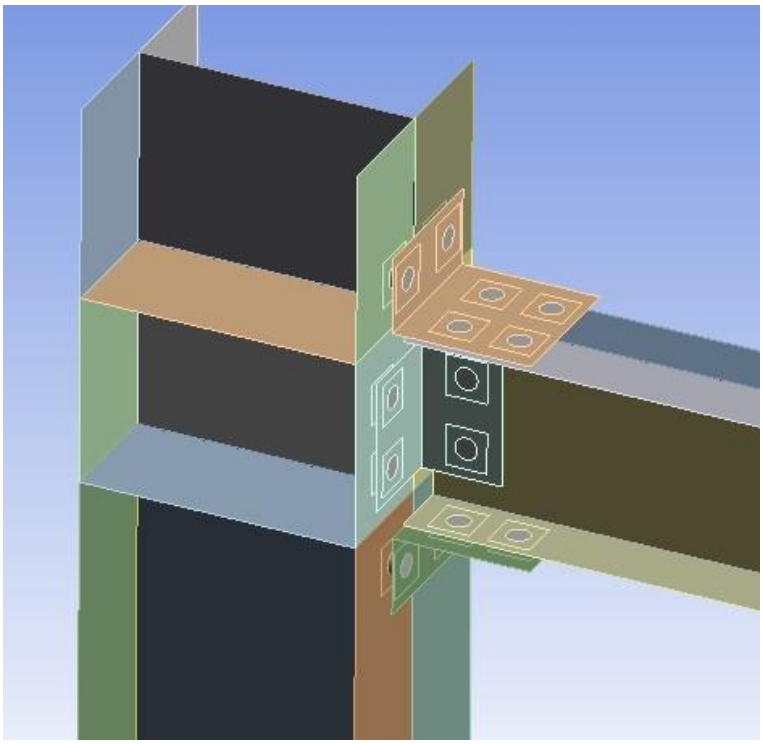

Figure 4. 7 Semi-Rigid (TSADWA) Connection Region of Steel Portal Frame in Shell Modeling

Although Azizinamini (Azizinamini, 1985) has already mentioned that they used heavy column sections to eliminate column panel zone effect as a contributing behavior factor, double stiffener plate adjusted to the beam flange line was added to guarantee PZ region stayed at elastic region.

For the meshing procedure, quadratic element order and 4 in (101.6 mm) element size are determined for optimized value after several attempts to find the ideal meshing technique. Around the holes, the number of division method is used, and rectangular shapes were projected on the angles to coordinate smooth transition between the edges for increasing mesh quality. It was set as the number of ten, and behavior type was selected hard as major property. The rest of them were left to default values. Elements and nodes numbers were 20700 and 64243, respectively.

Analysis settings in the static structural module were prepared to handle convergence problems during the analysis. Duration time was set as 4 sec. The first second was considered gravity load of structural steel frame with ‘Standard Earth Gravity’ for self-weight calculation and low quantity of overall pretension value 1000 lb (4448.221 N) was also used as clamping force while rest of it was left to a second time to neglect some convergence issue in the connection region. In the third second, the

distributed load was assigned on the beam as 100 lb/in (17512.684 N/m) in the vertical direction. In the last second, the lateral force was applied to the frame story level as a displacement value which was determined as 2.5% of story height related to top displacement value of life safety performance level according to FEMA-356 (FEMA-356, 2000). Left and right column supports were fixed, and out-of-plane movement was restricted to neglect lateral-torsional buckling.

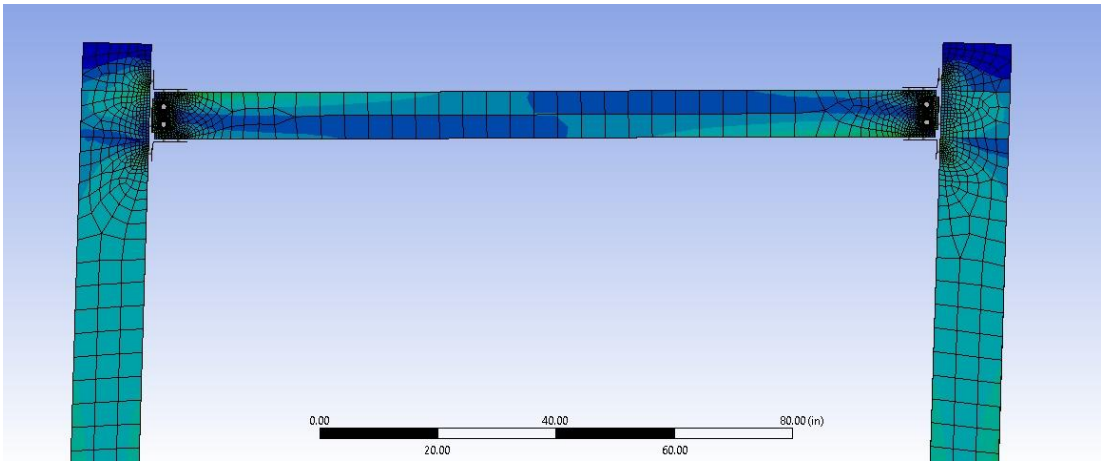

Figure 4. 8 Distribution of Equivalent Von – Mises Stress Contours

After running the analysis, Figure 4.8 shows deformed shape and stress distribution results of the frame at the end of analysis duration time (i.e., at fourth sec). Stress distribution demonstrates expected contours on the frame. On the other hand, stress contours on the beam also show correct force distribution that comes from the structural analysis method. Left bottom and top right angles were exposed to tension forces, and the other top and bottom angles were exposed to compression forces. Vertical and horizontal load combination increases rotation demand at the top angle of the right connection, and conversely, the same loading condition decreases rotation demand of the bottom angle of the left connection. Thus, as seen in Figures 4.8 and 4.9, these force distributions can closely be associated with the rotations in the PR connections. This relationship between the loading condition and movement of connections illustrates rotation capability of semi-rigid connection effects on overall frame behavior since although partially restrained connection enhances story drift value, its rotation capability concentrates the deformation on itself and ensues less strength loss on the adjacent structural members.

Therefore, if the semi-rigid connection has appropriate strength and rotation capacity under the earthquake loading condition, the push-over curve can be lengthened, and thus, the area of the curve can provide better energy dissipation.

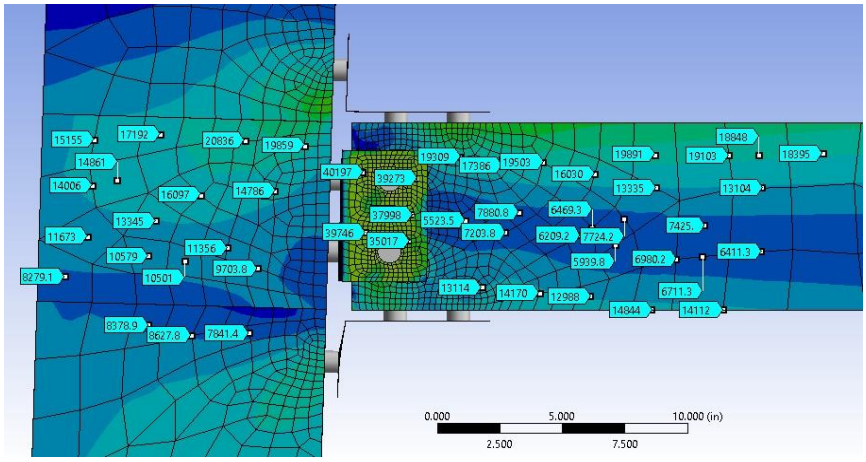

Figure 4. 9 Deformed Shape of Connection Region on the Left Column with the Stress Probes

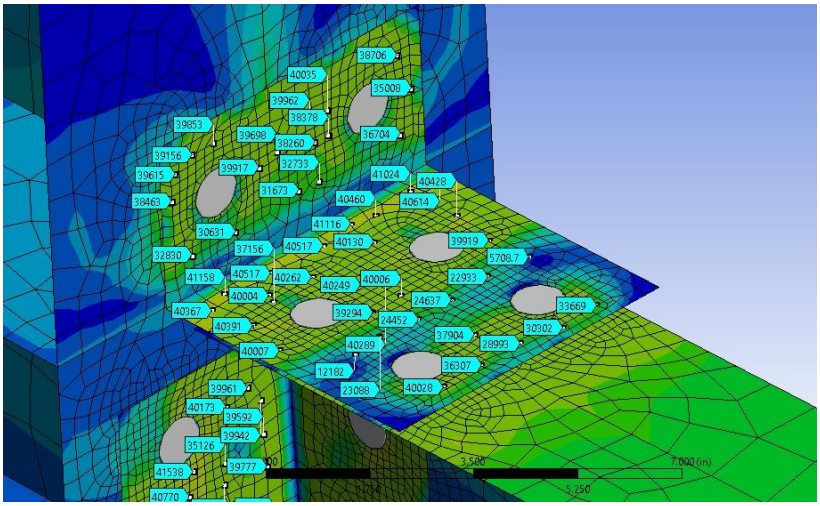

Figure 4. 10 Deformation Shape of the Top Angle with Stress Contours and Probes

Figures 4.9 and 4.10 shows panel zone region stayed at the elastic region, and its stress contours with probes make sure that nonlinearity was intensified in the connection region as expected. In this point, probes and contour transitions can also help to comprehend the partial restraint behavior of the TSADWA connection since, in

comparison to beam and column members, the deflected shape of the connection with its moment capacity demonstrates that where performance level of the frame is localized. Probes that have been on the figures can be observed considering yield stress value as 40000 psi (275.790 Mpa).

The right side (i.e., far side to the lateral loading) connection was chosen to examine the contours that display stress distribution of the top angle, which is exposed to a tension force, as seen in Figure 4.11. The top angle has almost the same level of straight stress lines along the section in the neighborhood of the corner and around the bolt holes, and high residual stress has taken place where the back of the top angle is connected to the column flange. Even if loading quantity and angle property are not directly the same, they both are exposed to the same loading characteristic, and therefore, their stress concentration lines and residual stress positions resemble as shown in Figures 4.11 and 4.12.

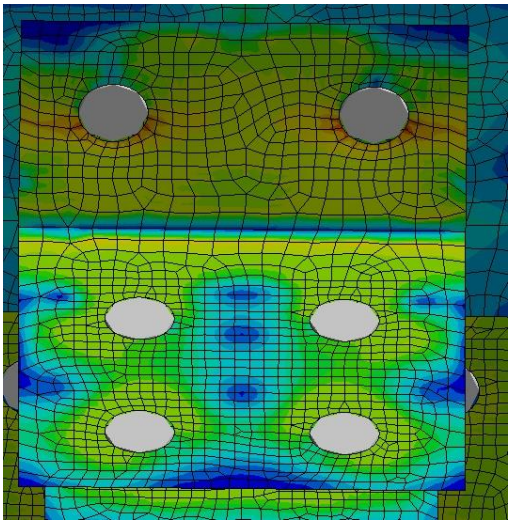

Figure 4. 11 Deformation Shape of the Top Angle with Stress Contours in the Right Column

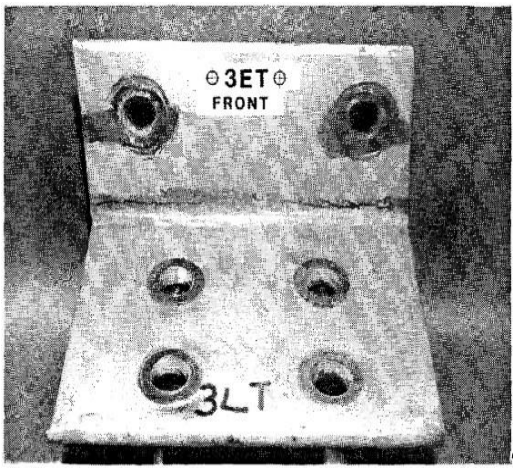

Figure 4. 12 Azizinamini's the Top Angle Specimen After Test

(Source: (Azizinamini, 1985))

After applied lateral load monotonically on the frame, a hysteresis analysis of the semi-rigidly connected steel portal frame was also evaluated to find out the reversal behavior of the frame by comparing the analysis results as seen in Figure 4.13. During this analysis in ANSYS, incremental displacement loading was conducted back and forth until reaching the top displacement value that is at 4 in (101.6 mm). All other modeling approaches and parameters with the same loading conditions were conserved as was done in push-over analysis. The number of steps was set as 40, and after the third-second lateral displacement was started to load by following ramped function on the frame. In the first round top drift value and at each turn, incremental value is carried out as 0.5 in (12.7 mm) until reaching the story drift limit.

At the end of the hysteresis analysis, 1439 iteration was performed, and it lasted approximately 9 hours through the direct analysis solver option. Even if hysteresis curve behavior doesn't represent strength and stiffness degradation, it still is a good example to examine the correlation between monotonic and cyclic loading under the bilinear isotropic material definition. Also, if knowing fatigue life tests were consisted, energy absorption capacities of the overall frame could have sensitively shown under reversal loading by using variable amplitude tests (High to low, low to high, and constant). In any case, however, it provides us with preliminary information about the repetitive motion of the frame.

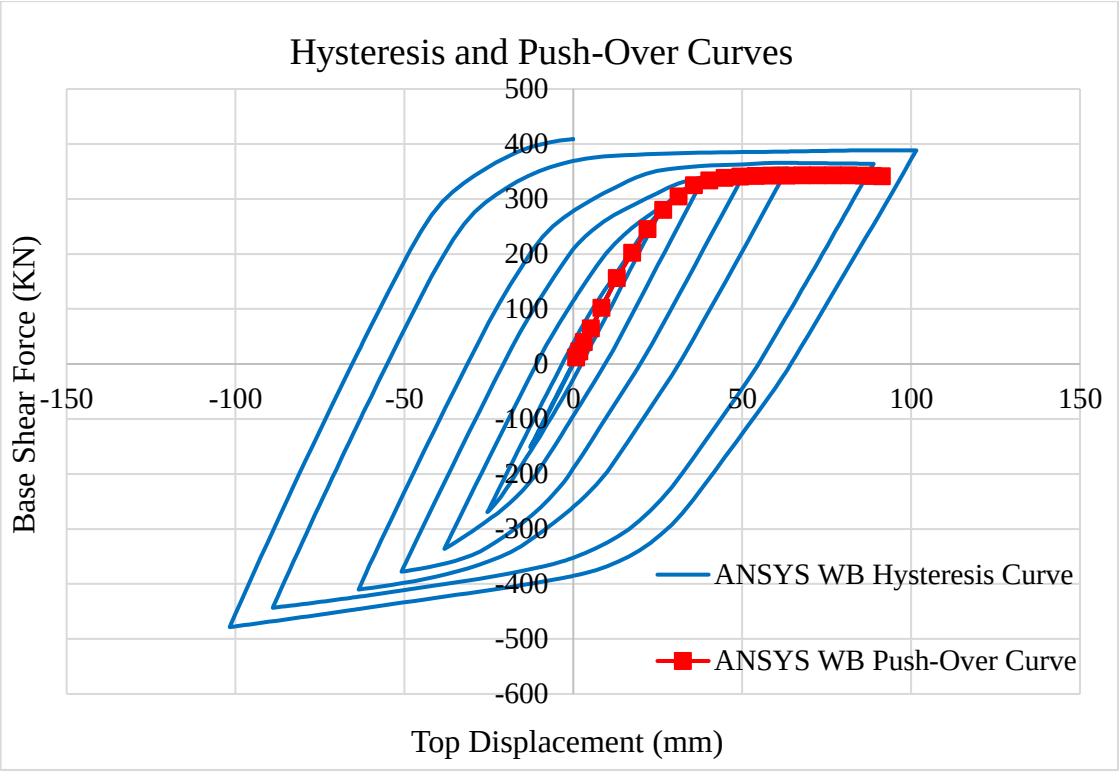

Figure 4. 13 Hysteresis and Capacity Curve of the Steel Portal Frames in ANSYS

After explaining major modeling points and obtaining analysis results in ANSYS, the SAP2000 modeling procedure was applied by following and considering sections 4.1,4.2 and 4.3. Beam and column members were defined, and the PZ region consisted of rigid link elements. Then, the semi-rigid connection was assigned between rigid link elements and endpoint of beam members as zero-length link elements by using multi-linear elastic link element property as illustrated in Figure 4.14. In chapter 2, Azizinamini's 8S10 connection model was elaborately explained and performed to focus on partially restraint behavior by eliminating the rest of the member affects as much as possible as intended in the experimental study. Thus, obtained moment-rotation curve was used in the selected link element property, and the frame was modeled as shown in Figure 4.15.

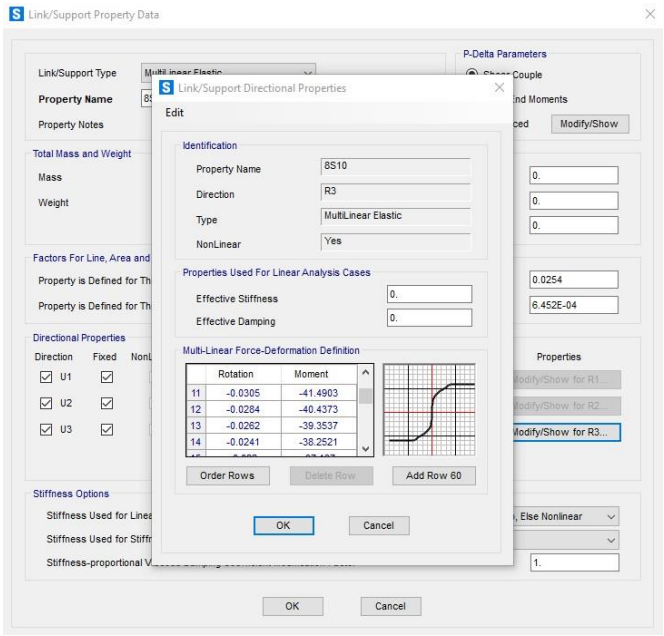

Figure 4. 14 Multi-Linear Moment-Rotation Relationship for 8S10 Semi-Rigid Connection, KN.m-Rad.

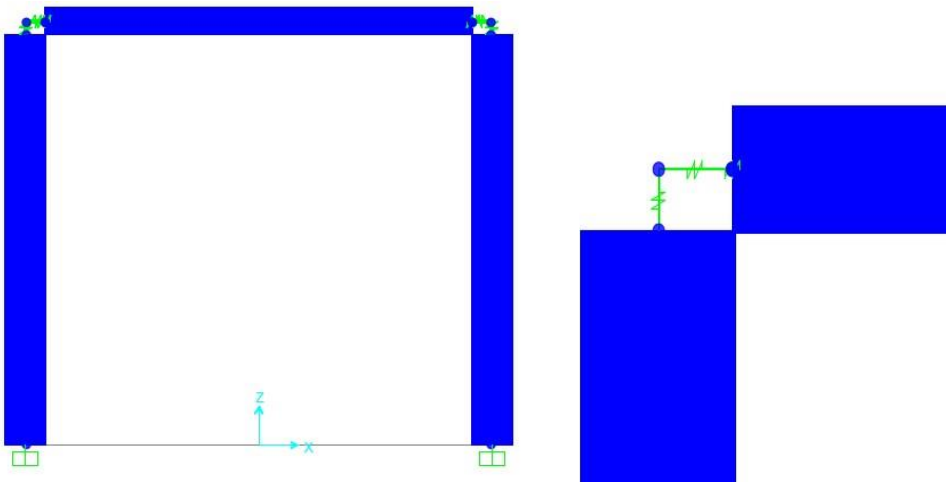

Figure 4. 15 Representation of A Semi-Rigid Steel Portal Frame

When the modeling and analysis process is completed for both ANSYS and SAP2000, their backbone curves can be obtained and compared to rigid and pinned ones. This comparison is used to bring to light the effect of the semi-rigid connection on the frame. Figure 4.16 shows that the capacity curve of the TSADWA semi-rigid connection falls between rigid and pinned connection behavior as expected. Also, ANSYS and SAP2000 capacity curves continue along the curve in perfect harmony until the target top displacement value, which is determined as 3.6 in (91.44 mm) FEMA-356, allows for a

2.5 percent drift allowance (FEMA-356, 2000). Thus, due to the lack of convenient experimental semi-rigid frame samples in the literature, the steel portal frame example is conducted to compare PR connection models with each other, which were performed in ANSYS and SAP2000. Results, supported by ANSYS' sufficiently detailed analysis capability, showed that developed approaches are convenient to evaluate the frame analyses with moment-rotation curves of the connections in the related link elements in SAP2000.

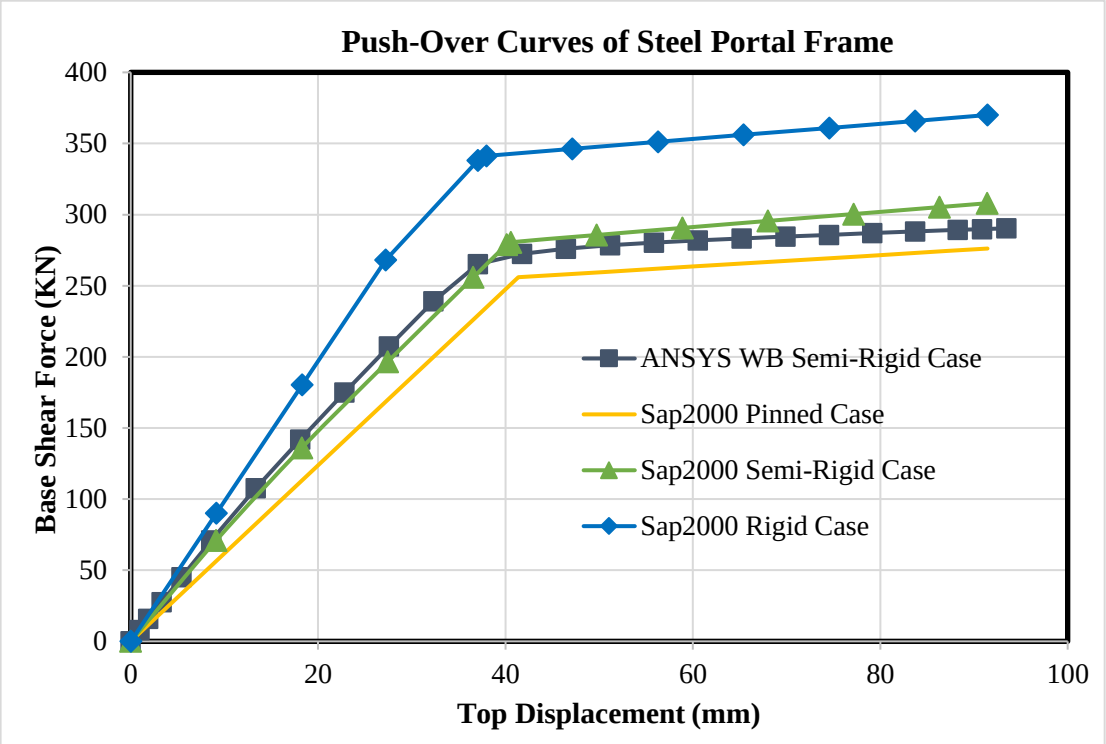

Figure 4. 16 Comparison of Push-Over Curves Including Rigid, Pinned and TSADWA Semi-Rigid Connections.

Example 2. Ten Story – Three Bay PR Steel Frame

The three-bay, ten-story steel frame is considered as the design example (Doğan, 2010). The dimensions of the frame are taken place with 5m width for each span, L_{bay},5m, and 3.5m height for each story, h_i. Modeling representations are shown in Figure 4.17. The frame is subjected to gravity loading of 50 KN/m on the beams of roof level and the beams of each floor. Fixed supports are used for the connection of the columns to the foundation. In the frame, W610x53 exterior and W610x113 interior profiles for columns

and W460x68 profile for beams were chosen, and A36 class mild steel was used as steel type. All 2D planar frame analysis features and performance limit criteria were adopted, as was done in example 1. However, AISC based partially restrained moment–rotation definitions were used in this example to assign it to the structural frame model. The purpose of using a code-based PR connection approach is to parametrically observe the effects of connection components (i.e., change in connection strength and stiffness values) that are consisted based on its adjacent members' capacity that leads to getting the most appropriate range of the semi-rigid connection without direct modeling need of the TSADWA or other types of the PR connections. According to AISC360-16 (AISC 360-16, 2016) some connection parameters should be defined to specify limits of connection on the graph as follows:

- M_{yc} and θ_{yc} are the yield moment and rotation capacity of the connection,
- M_{pc} and θ_{pc} are the plastic moment and rotation capacity of the connection,
- M_{uc} and θ_{uc} are the ultimate moment and rotation capacity of the connection.

As explained before in the connection classification section, the moment-rotation of the connection model should be plotted by considering strength, stiffness, and ductility. Thus, depending on the description of the specification, connection graphs have been plotted, as shown in Figure 4.18.

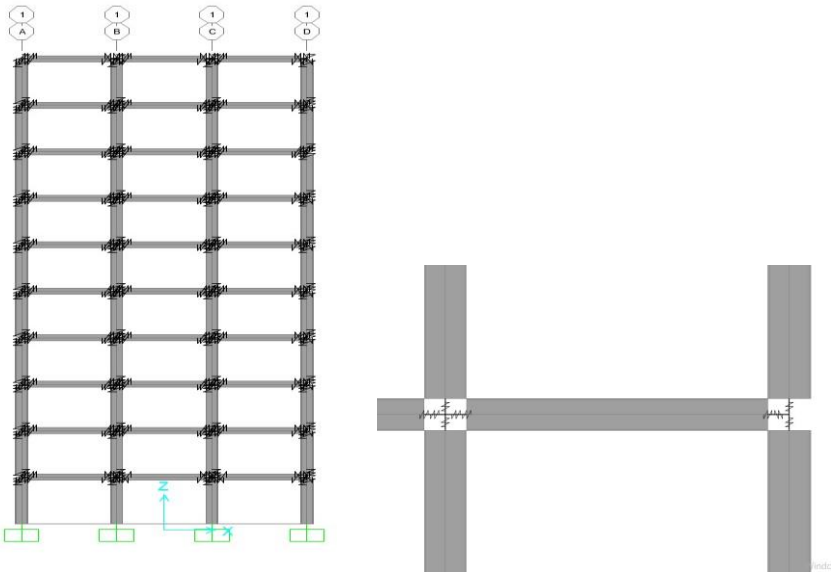

Figure 4. 17 Representation of the Frame and PR Connection Model

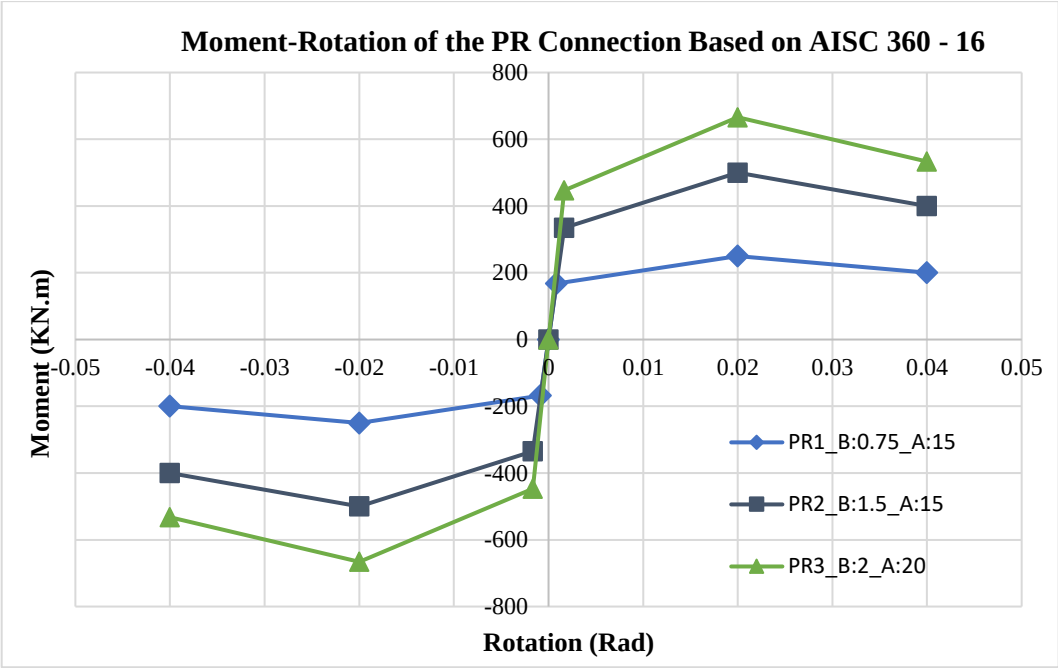

Figure 4. 18 PR Connection Models with Different Strength and Stiffness Values

By taking reference point to plastic moment capacity of the beam, M_{pb}, strength capability of the connection was determined by comparing it with $M_{pc,}$ and their ratio is represented with β in change 0.75, 1.5, and 2. When the β value increases, the connection strengthens as defined by Eq. 4.3. θ_{pc} rotation value of 0.02 rad was accepted based on AISC definition to represent moment – rotation of peak resistance level. θ_{uc} is also accepted as 0.04 rad based on AISC 341-16 (AISC 341-16, 2016) to consider the example of the frame in special moment frame (SMF) for providing connection ductility criteria. Its ultimate moment capacity, i.e., M_{uc}, is determined as equal to the resisting strength of the connection has dropped to 0.8Mpc (AISC 360-16, 2016). Lastly, M_{yc} of the connection was assumed to be equal to 67% of M_{pc} according to the studies that have been published in the literature.

Only parameter θ_{yc} needs to be figured out to complete the moment-rotation graph of connections by putting the curve into the structural steel frame. In this point, stiffness parameter α that is the initial connection stiffness value in the range between 2 and 20, is used by calculating Eq. 4.4 to specify yield rotation value, θ_{yc}, as mentioned in chapter 1. Thus, stiffness parameter α between 2 to 20 for the partially restrained (or semi-rigid) connection range is arranged to demonstrate the effect it on the frame capacity.

A numerical example to find the parameters of all the three types of connections are given in Table 4.1, in which the graph of that selected connection can be seen from Figure 4.18.

Table 4. 1 Material and Section Properties of the Beam,W460x68

SteelGrade: A36	(250 Mpa yield; 450 Mpa Tensile Strength)
I	711.1428 in^4 (2.960x10^8 mm^4)
E	29 ksi (199948 Mpa)
L_{bay}	5 m
M_{pb}	332.851 KN.m
K_{beam}(EI/L)	11780800 N.m

$$M_{pc} = M_{pb}\,\beta \tag{4.3}$$

$$\theta_{yc} = M_{yc} / \alpha\,(EI/L) \tag{4.4}$$

Based on the above beam stiffness and strength values, parameters of three connection types (PR1, PR2, PR3) can be calculated with different α (15;20) and β (0.75;1.5;2) values to observe semi-rigidity on the example of a frame. The calculated 'PR1' connection that has been in Figure 4.18 can be seen elaborately in Table 4.2.

Table 4. 2 Moment- Rotation Values of the PR1 Connection

Type: PR1	**β:0.75**		
	α:15		
	Moment (KN.m)	**θ (Rad)**	
M_{uc}	-200	-0.04	**θ_{uc}**
M_{pc}	-250	-0.02	**θ_{pc}**
M_{yc}	-167.5	-9.43E-04	**θ_{yc}**
Origin	0	0	**Origin**
M_{yc}	167.5	9.43E-04	**θ_{yc}**
M_{pc}	250	0.02	**θ_{pc}**
M_{uc}	200	0.04	**θ_{uc}**

After connection, parameters are explained, and models are obtained. The rest of the modeling and analysis parameters of SAP2000 software were adopted again by taking into account sections 4.1,4.2 and 4.3. Push-over curves were plotted for each connection model to compare them with rigid ones, as shown in Figure 4.19.

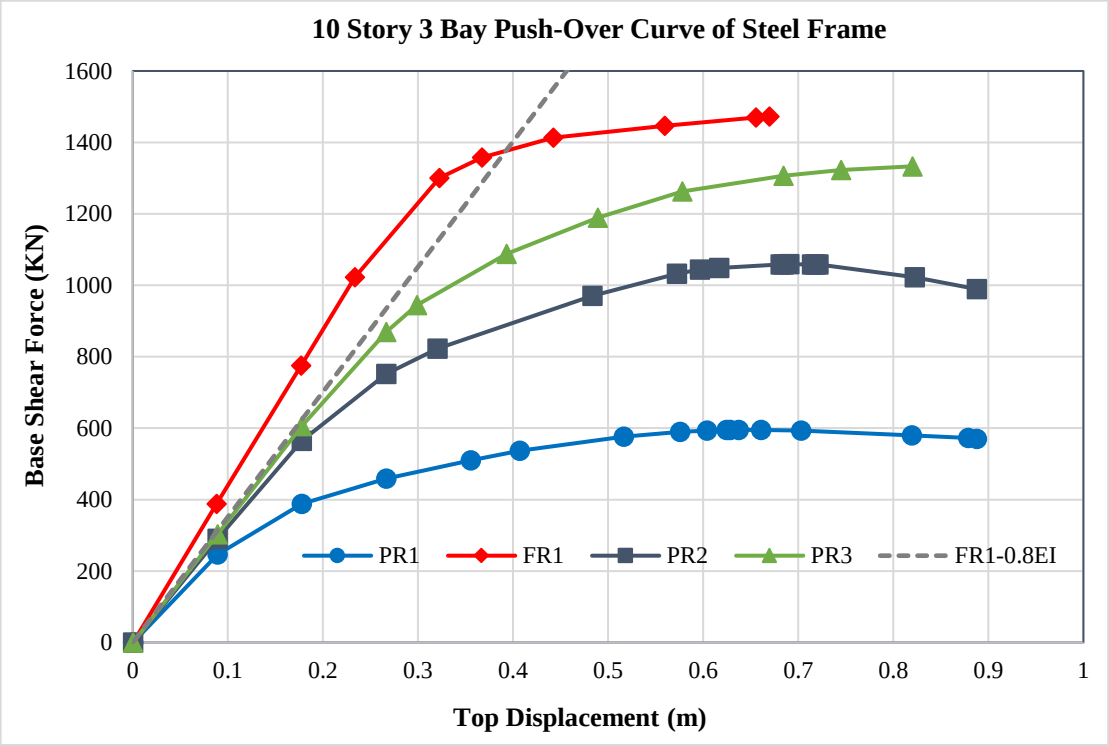

Figure 4. 19 Capacity Curves of the Frames with Different Stiffness and Strength values of PR Connections.

As seen in the results of the push-over analysis, as the stiffness and strength of the connection increase, the max shear resistance of the structure increases, but, on the other hand, the deformation capacity decreases. In PR1 and PR2 connection case where the value of α is kept the same, but the value of β changes, Although the length of the curves is almost the same, it can be observed that the increase in the base shear capacity is due to the increase in the strength of the connection, PR2, and its curve shows higher ductile capacity. Besides, for PR3 connection's model, although connection strength was doubled of the beam plastic strength, M_{pb}, and stiffness, α, was raised until semi-rigid up-limit value, its curve is closely related to rigidly connected frame behavior and, however, it still shows having higher flexibility on the frame behavior by preventing moving directly forward to power depletion due to strength reduction in the structure.

Meanwhile, the capacity curve of an ideally rigid connected frame shows that rigid connection assumption can be misleading in some cases. Since performed analyses, for this example, presented rigid connection several times stiffer than beam stiffness (EI/L) and strength capacity also extremely higher than plastic moment capacity of the beam, was needed to obtain almost same capacity curve with rigid one. Reduced stiffness of column, $0.8E_cI_c$, is also applied to the FR1 connected frame by decreasing the initial tangent of the capacity curve to get closer to the PR3 connected frame's curve. This approach is adopted since steel structural frames in engineering design life contain some stability requirements (i.e., in this case, use part of the direct analysis method) to show up the design capacity of the rigidly connected frames, especially in the linear range. Even if semi-rigid connections are not directly part of this approach, it is still affected relatively by the design principles; thus, the capacity curve of the 'FR1-$0.8E_cI_c$' frame differentiates from the full-rigidly connected FR1 frame. Comparison of the base shear resistances along the path of curvature reveals that the FR1 connected frame with reduced stiffness shows convergence to the PR3 connected frame at the low level of the initial stiffness range. However, after that, the semi-rigidly, PR3, the connected frame starts to divergence towards the end of the initial slope, relative to the rigid ones, by following its second stiffness path to reach the nonlinear capacity of the frame under its connection efficiency. In the light of overall analyses carried out for semi-rigidly connected frames with different properties results that instead of directly attempting to ideally pinned or rigid assumptions of the connections in engineering design life, connection stiffness, and strength analysis, based on the specifications and codes, should carefully be taken into account to reveal actual connection capacity. The curve also shows that frame behavior has optimization capability through semi-rigid connections within changing its strength and stiffness. In conclusion, if earthquake demands are to be resisted at the desired performance level, frame behavior can be managed due to semi-rigid connections, provided giving more economical and reliable results.

CHAPTER 5

SUMMARY AND CONCLUSION

5.1. Summary

The thesis's first chapter began with a general introduction and included a brief history of the connections. The properties of partially restrained connection forms, commonly called semi-rigid, were then identified and represented. The AISC code descriptions were used to describe and detail the general classification scheme for connection types and their application ranges. Previous finite element and frame analyses which various researchers conduct, were investigated, and basic definitions and details of these analyses were presented following the sequence of events in the thesis.

In the second chapter of this thesis, using the ANSYS FE software, the nonlinear finite element modeling of semi-rigid connection stages was described, and experimental analysis was adapted to a finite element simulation to check the adequacy of the connection model. In the scope of the thesis Azizinamini's (Azizinamini, 1985) top and seat angle with double web angle (TSADWA) semi-rigid connection model was chosen due to its easy implementation feature. The connection model process was provided, along with the details needed for the nonlinear finite element analysis. The models' general structure, element types, friction coefficients, pretension values, and material models were among them. The experimental studies were modeled, analyzed, and presented. The nonlinear finite element modeling results and comparisons on the TSADWA connection are presented in the next chapter.

The third chapter of this thesis focused on the simplified mathematical models developed by various researchers. The corresponding model definitions are briefly explained with necessary information. The linear, multi-linear, polynomial models are discussed. Among these models, Frye and Morris's (Frye & Morris, 1975) polynomial model was used to revealing the correlation of mathematical model with FE model and experimental results. The mathematical model compared to the obtained moment-rotation results demonstrates that semi-rigid connections can be modeled in the finite element

environment with the help of the curve-fitting model by providing accuracy. The study's main goal on semi-rigid connections until the end of this section is to eliminate the need for experimental research by assuring reliable results and a practical approach for the PR connection modeling.

The seismic performance of 2-D steel frames was assessed using FEMA-356 procedures in the fourth chapter. Nonlinear static analysis (push-over) was chosen to present how a semi-rigid connection affects the frame under earthquake loading. During the frame analysis process, semi-rigid TSADWA connection models that were modeled in ANSYS and also based on AISC 360-16 were assigned to beam-column connections. In order to demonstrate connection characteristics on the frame, the push-over analyses of semi-rigidly connected frames and rigidly connected frames were compared.

5.2. Conclusion

In today's structural engineering world, the use of semi-rigid connections is in limited quantity. The structural research of these types of connections and the reliability of the analysis are the remaining issues with these connections in terms of use in engineering practice. Therefore, one of the aims of this study is to see if today's advanced finite element software will support such a simulation by carefully modeling nonlinearities in the connection region. The results of finite element simulations of moment-rotation curves were compared to experimental results. This comparison revealed uncertain parameters of the connection region by considering literature information and codes. The mathematical model for the TSADWA connection type is added to the analyses for further verification and eliminating the need for experimental research. Frame analyses of semi-rigid (TSADWA) connection was evaluated first to demonstrate analysis effectiveness by comparing with detailed finite element model (ANSYS) due to lack of experimental information on the semi-rigidly connected steel frames. Then, AISC specification is used to show the PR connection effect on the push-over analysis by considering stiffness, strength, and ductility criteria.

The following are the main conclusions of this study:

A detailed finite element model of the PR connection gives physically consistent representations of the deformed shape of the connection region. The starting stiffness of the moment–rotation curves, which was calculated using finite element simulations, was lower. According to experimental data, the researchers employ highly strong beam sections to ensure a specimen connection's failure before the connecting beam yields. Furthermore, the selected column sections are ensured not to deform beyond the elastic range (using thick flanges and stiffeners for neglecting the PZ effect). This physical behavior is adopted by the presented connection and frame models, with the ANSYS, in this thesis.

Example results of steel portal frame clearly showed that SAP2000 could be used effectively for semi-rigidly connected frame models. Selected link elements to consist of the model and analyze the frame, with the appropriate assumptions and simplifications from literature, standards, and specifications, are suitable compared to the ANSYS PR connected (TSADWA) frame model.

Stiffness and plastic moment capacity was chosen as the connection parameters to characterize semi-rigid connections in the scope of the thesis. According to the examples, the capacity curves were primarily affected by the connection's moment capacity. There is a direct proportional relationship between the moment capacity of the connection and the yield slope of the connection in the studies circumstances.

Results of example 4.2 demonstrate that how semi-rigidly connected frames are exposed to change due to the change in their connection characteristics. For instance, a PR1 and PR2 connection comparison shows that, using the same connection stiffness value, α. In contrast, the strength coefficient value, β, is two times the other, and max resistance capacity of base shear shifted from 600 KN to 1100 KN by following the same tangent. And this ends up with a nearly 85% increase of the max value of the capacity curve on the ordinate axis. On the other hand, in the PR2 and PR3 connection, max base shear value is around a 10% increase due to the smaller difference between β values, as shown in Figure 4.18. Also, results revealed that the capacity of the semi-rigid connection has a limited effect on frame behavior when the connection stiffness is close to the upper limit value of the semi-rigid boundary condition.

All of the pushover investigations indicated that the stiffness of the connection contributes substantially less to the lateral load-bearing capacity than the connection's

plastic moment capacity. When the plastic moment capacity ratio of semi-rigid connection to beam, β, was equal to 2, the push-over curve of the frame is getting closer to the rigidly connected one. However, they are still far from the same for base shear capacity. Therefore, the connection (PR3) has also revealed that the idealized connection approach cannot be accurate without considering connection strength and rotation capacity. It can mislead from the point of view of contribution to the pushover curves.

When analyzing frames with semi-rigid connections, the designer should pay close attention to the serviceability criteria since lateral deformations of semi-rigidly connected frames are much greater than those of rigid frames. Therefore, target displacement of frames was primarily a consideration for semi-rigid connections to specify the base shear-displacement capacity. If structural optimization is desired, the moment-rotation of the semi-rigid connection can be modified by repeating the entire process concerning the required sensitivity of the capacity curve focused on base shear and top displacement values.

As a result, this thesis intended to reveal semi-rigid connection models and their usage on the steel frames with the help of advanced computer software without the need for experimental research. Understanding the effectiveness of PR connection behavior can propose a reliable and practical methodology for the analysis process. The importance of appropriate analysis for necessary studies on connection details should be conducted to obtain desired performance, serviceability, and optimum member requirements for seismic areas.

5.3. Future Recommendations

The following suggestions can be made based on this research:

- It is possible to investigate the efficiency of frames with different types of semi-rigid connections with performance analysis.
- Semi-rigid connection models should be used in dynamic time-history analyses of the same set of frames.
- A study on optimizing semi-rigid connection frames can be performed for the specified performance level.

- Modeling panel zones can be placed in the inelastic region, in addition to semi-rigid connections, to increase joint efficiency and to see the combined effect on the system behavior.

REFERENCES

AISC 341-16. (2016). *Seismic Provisions for Structural Steel Buildings.* Chicago

AISC 360-16. (2016). *AISC 360-16, Specification for Structural Steel Buildings.* Chicago.

Akgönen, A. İ., & Güneş, B. (2017). Alın Levhalı Moment Birleşimlerin Sonlu Elemanlar İle Analizi. *AKU J. Sci. Eng.*, 646-657.

ANSYS INC. (2015). *ANSYS User Manual Version 16.0.* Canonsburg, Pennsylvania.

ASTM A325 & A490. (2004). *ASTM A325 & A490, Specification for Structural Joints Using ASTM A325 or A490 Bolts.* Chicago.

ATC-40. (1996). *ATC-40, Seismic Evaluation, and Retrofit of Concrete Buildings Vol 1*. California: Seismic Safety Commission.

Azizinamini, A. (1985). Cyclic Characteristics of Bolted Semi-Rigid Steel Beam to Column Connections. The *University of South Carolina*.

Chan, S. L., & Chui, P. T. (2000). Nonlinear Static and Cyclic Analysis of Steel Frames with Semi-Rigid Connections. *Elsevier*.

Chen, W. F. (2000). Practical Analysis for Semi-Rigid Frame Design. *World Scientific*.

Chen, W. F., & Kishi, N. (1989). Semi-Rigid Beam to Column Connections: Data Base and Modeling. *Journal of Structural Engineering*, 105-119.

Chen, W. F., & Lui, E. M. (1991). *Stability Design of Steel Frames.* Boca Raton, FL: CRC Press.

Chen, W. F., Kishi, N., & Komuro, M. (2011). *Semi-Rigid Connections Handbook.* J. Ross Publishing.

Citipitioglu, A. M., Haj-Ali, R. M., & White, D. W. (2002). Refined 3D Finite Element Modeling of Partially Restrained Connections Including Slip. *Elsevier*, 995-1013.

CSI Analysis Reference Manual. (2017). Analysis Reference Manual. The USA.

Danesh, F., Pirmoz, A., & Daryan, A. S. (2006). Effect of Shear Force on the İnitial Stiffness of Top and Seat Angle Connections with Double Web Angles. *Elsevier* , 1208-1218.

Deierlein, G. G., Reinhorn, A. M., & Willford, M. R. (2010). Nonlinear Structural Analysis For Seismic Design. *NEHRP Seismic Design Technical Brief No. 4*, 1-32.

Doğan, E. (2010). OPTIMUM DESIGN OF RIGID AND SEMI-RIGID STEEL SWAY FRAMES, INCLUDING SOIL-STRUCTURE INTERACTION. 1-262.

Elnashai, A. S., & Elghazouli, A. Y. (1994). Seismic Behaviour of Semi-Rigid Steel Frames. *J. Construct. Steel Research*, 149-174.

Erdem, H. (1999). Yarı Rijit Bağlı Düzlemsel Çerçevelerin Nonlinear Analizi. *Fen ve Mühendislik Dergisi*, 1-12.

Faella, C., Piluso, V., & Rizzano, G. (1999). *Structural Steel Semi-Rigid Connections Theory, Design, and Software.* Boca Raton, Florida: CRC Press LLC.

Fakih, K. A., Chin, S. C., & Doh, S. I. (2018). The behavior of Extended End-Plate Steel Beam to Column Connections. *The Open Civil Engineering Journal*, 250-262.

FEMA-356. (2000). *FEMA 356, Federal Emergency Management Agency*. Washington.

Frye, M. J., & Morris, G. A. (1975). Analysis of Flexible Connected Steel Frames.

Hayalioglu, M. S., Degertekin, S. Ö., & Görgün, H. (2004). Design of Semi-Rigid Planar Steel Frames According to Turkish Steel Design Code. *Journal of Engineering and Natural Sciences*, 101-114.

Hsieh, S. H., & Deierlein, G. G. (1990). Nonlinear Analysis of Three-Dimensional Steel Frames with Semi-Rigid Connections. *Computers & Structures*, 995-1009.

Johnson, D. H. (2001). *Principles of Simulating Contact Between Parts Using Ansys.* Mallet Technology Inc.

Jones, S. W., Kirby, P. A., & Nethercot, D. A. (1980). Effect of Semi-rigid Connections on Steel Column Strength.

Jones, S. W., Kirby, P. A., & Nethercot, D. A. (1983). The Analysis of Frames with Semi-Rigid Connections. *Journal of Constructional Steel Research*.

Koieala, B., & Suwal, R. (2020). Seismic Performance Evaluation of Steel Frame Structure Considering Semi-Rigid Connections. *American Journal of Sciences and Engineering Research*, 44-51.

Leon, R. T. (2017). *Handbook of Structural Steel Connection Design and Details.* Mc Graw Hill Education.

Mahin, S. A. (1998). Lessons from damage to steel buildings during the Northridge earthquake. *Elsevier Science*, 261-270.

Miri, M., & Naghipour, M. (2009). Panel Zone Effects on Special Steel moment-resisting Frames According to the Performance-Based Design. *World Academy of Science*, 925-931.

National Institute of Standards and Technology. (2017). Guidelines for Nonlinear Structural Analysis for Design of Buildings. *NEHRP*, 145.

Nguyen, C. P., & Kim, S. E. (2014). Nonlinear inelastic Time-History Analysis of Three Dimensional Semi-Rigid Steel Frames. *Elsevier*, 192-206.

Pirmoz, A., & Danesh, F. (2009). The Seat Angle Role on Moment-Rotation Response of Bolted Angle Connections. *Electronic Journal of Structural Engineering*, 73-79.

Pirmoz, A., & Gholizadeh, S. (2007). Predicting of Moment-Rotation Behavior of Bolted Connections Using Neural Networks.

Prabha, P., Rekha, S., Marimuthu, V., Saravanan, M., Palani, G. S., & Surendran, M. (2015). Modified Frye–Morris polynomial model for double web-angle connections. *Springer*, 295-306.

Sagiroglu, M., & Aydin, A. C. (2015). Design and Analysis of Steel Space Frame with Semi-Rigid Beam-to-Column Connections Using Stiffness Method. (s. 1405-1421). Steel and Composite Structures.

Singh, R., & Lui, E. M. (2014). Design of PR Frames with Top and Seat Angle Connections Using the Direct Analysis Method. *Advanced Steel Construction*, 116-138.

Surovek, A. E., White, D. W., & Leon, R. T. (2005). Direct Analysis for Design Evaluation of Partially Restrained Steel Framing Systems. *J. Struct. Eng.*, 1376-1389.

Şeker, S., Doğan, E., & Kozanoğlu, C. (2017). Yarı Rijit Çelik Çerçevelerin Stokastik Arama Yöntemleri Kullanılarak Optimum Boyutlandırılması. *Celal Bayar University Journal of Science*, 785-795.

Weynand, K., Jaspart, J. P., & Steenhuis, M. (1998). Economy studies of steel building frame with semirigid joints. *Journal of Constructional Steel Research*.

.